Title

An application of the water footprint assessment to optimize production of crops irrigated with saline water: A scenario assessment with HYDRUS

Journal

Agricultural Water Management, 208(C)

ISSN

0378-3774

Authors

Karandish, F
Šimůnek, J

Publication Date

2018-09-30

DOI

10.1016/j.agwat.2018.06.010

Peer reviewed

Agricultural Water Management 208 (2018) 67–82

Contents lists available at ScienceDirect

Agricultural Water Management

journal homepage: www.elsevier.com/locate/agwat

An application of the water footprint assessment to optimize production of crops irrigated with saline water: A scenario assessment with HYDRUS

Fatemeh Karandish[a,*], Jiří Šimůnek[b]

[a] Water Engineering Department, University of Zabol, Zabol, Iran
[b] Department of Environmental Sciences, University of California Riverside, Riverside, CA 92521, USA

ARTICLE INFO

Keywords:
Economic water productivity
Grey water footprint
Maize
Numerical simulations
Salt stress
Water deficit
HYDRUS

ABSTRACT

Agriculture, due to a growing scarcity of fresh water resources, often uses low-quality waters for irrigation, such as saline waters. However, unmanaged applications of such waters may have negative environmental and economic consequences. Based on the concept of the water footprint (*WF*), a measure of the consumptive and degradative water use, the field-calibrated and validated HYDRUS (2D/3D) model was applied to find optimal management scenarios (from 1980 different evaluated scenarios). These scenarios were defined as a combination of different salinity rates (SR), irrigation levels (IL, the ratio of an actual irrigation water deth and a full irrigation water depth), nitrogen fertilization rates (NR), and two water-saving irrigation strategies, deficit irrigation (DI) and partial root-zone drying (PRD). The consumptive *WF* was defined as the crop water consumption divided by the crop yield. The grey *WF* was calculated for the N fertilizer and defined as the volume of freshwater required to dilute nitrogen (N) in recharge so as to meet ambient water quality standards. Simulated components of water and solute dynamics were used to calculate criteria indices, which were divided into two groups: (a) environmental indices, including the degradative grey water footprint (*GWF*) and the apparent N recovery rate efficiency (*ARE*), and (b) economic indices, including economic water (*EWP*) and land (*ELP*) productivities. While significant improvements of 3.9–59.2%, 0.1–165.8%, and 0.01–166.5% in *ARE*, *EWP*, and *ELP*, respectively, were obtained when NR varied within the range of 0–200 kg ha^{-1}, changes in these indices were relatively minor when NR was higher than 200 kg ha^{-1}. At a given NR, *GWF* tends to increase considerably by up to 180% when DI-crops are subject to low-intermediate salt (SR $<$ 7 dS m^{-1}) and water (IL $>$ 70%) stresses. This is at the expense of up to a 55% reduction in *ELP* and up to a 120% increase in *EWP*. With N uptake 0.2–17.3% higher, PRD seems to be a more viable agro-hydrological option than DI in reducing a pollutant load into regional aquifers as well as in sustaining farm economics. The entire analysis reveals that the PRD strategy with N-fertilization rates of 100-200 kg ha^{-1}, a moderate salinity stress (SR $<$ 5 dS m^{-1}), and irrigation levels of 60–90% represents the best management scenario. It can be concluded that, while there is a substantial need for rescheduling irrigation and fertilization managements when crops are irrigated with saline waters, HYDRUS modeling may be a reliable alternative to extensive field investigations when determining the optimal agricultural management practices.

1. Introduction

It has been well documented that groundwater pollution induced by the agricultural sector poses a serious and widespread environmental threat to Iran (e.g., Karandish et al., 2016), California (e.g., Harter and Lund, 2012), and many other countries. In Iran, after the 1979 Islamic revolution, the government implemented several new agricultural policies aimed at achieving national food security through increased domestic productivity and self-sufficiency of staple crops (Karandish and Hoekstra, 2017). The construction of irrigation and drainage networks and enhanced applications of organic/inorganic fertilizers were among these policies. While Iran's policy on agricultural self-sufficiency satisfied growing demands for food and raw materials, ill-thought-out agricultural practices resulted in adverse environmental consequences. The alteration of the balance of soil N compounds through excessive uncontrolled applications of N-fertilizers above optimal amounts and without considering crops N requirements led to significant groundwater pollution (Zhu et al., 2005; Thompson et al., 2007; Dudley et al., 2008; Burow et al., 2010; Dahan et al., 2014; Karandish et al., 2016).

Nitrate vulnerability may be of particular interest in water-scarce

* Corresponding author.
E-mail addresses: Karandish_h@yahoo.com, F.Karandish@uoz.ac.ir (F. Karandish).

https://doi.org/10.1016/j.agwat.2018.06.010
Received 1 March 2018; Received in revised form 4 June 2018; Accepted 7 June 2018

regions where crops need to be produced with minimal fresh water. In these regions, there is room for savings of fresh water if crops receive less irrigation water during their growing season (Karandish and Šimůnek, 2016a). In this regard, many researchers have investigated the economic and environmental consequences of applying deficit irrigation (DI) (Payero et al., 2006; Klocke et al., 2004; Stone, 2003) or partial root-zone drying (PRD) (Dry and Loveys, 1998; Kang and Zhang, 2004; Kirda et al., 2004; Shao et al., 2008; Tang et al., 2005; Karandish and Šimůnek, 2016a, 2016b). They mostly concluded that, while significant economic losses could be expected under DI, PRD may produce water savings without a significant decrease in yields. While crops are exposed to the water stress under both DI and PRD, the way the stress is applied under PRD may produce better results. A regular alternation of irrigated and non-irrigated sides of the crop under PRD results in the secretion of root-generated Abscisic Acid (ABA) (Schachtman and Goodger, 2008), which is transported to shoot regulating stomata of the leaves. Such regulation reduces crop water losses through stomata, while maintaining crop CO_2 adsorption at the favorable level (Kang and Zhang, 2004), which consequently results in a higher crop water use efficiency compared to DI, or even FI (Karandish and Šimůnek, 2016a).

Although irrigation with saline waters may be another alternative to using fresh water in the agricultural sector (Pereira et al., 1995), this may lead to serious economic and environmental losses if not managed properly (Yurtseven and Sönmez, 1992; Mer et al., 2000; Zhu et al., 2005; Thompson et al., 2007; Corwin et al., 2007; Dudley et al., 2008; Roberts et al., 2009; Burow et al., 2010; Dahan et al., 2014). Water or salinity stresses may reduce crop N uptake (Karandish and Šimůnek, 2017; Ramos et al., 2012) and lead to higher nutrient loads into aquifers as a byproduct of N leaching out of the root zone (Zhu et al., 2005; Thompson et al., 2007; Dudley et al., 2008; Burow et al., 2010; Dahan et al., 2014; Karandish et al., 2016). If fresh water is applied, N leaching may be lower under PRD than under DI due to a higher crop N recovery (Kang and Zhang, 2004; Kirda et al., 2005; Li et al., 2007; Wang et al., 2009; Hu et al., 2009; Wang et al., 2012; Karandish and Šimůnek, 2017), which could translate into lower groundwater contamination. Even so, no earlier studies have ever attempted to find the optimal combination of N fertilization rates and applied water levels under PRD irrigated with saline water.

The degradative grey water footprint (*GWF*) may be an appropriate measure to assess new adjustments to the N fertilization rate under combined water and salinity stress conditions. Considered an indicator of the pollution assimilative capacity (Chukalla et al., 2017), the *GWF* is defined as the volume of freshwater required to dilute a load of pollutants so as to meet ambient water quality standards (Hoekstra et al., 2011). The *GWF* of the crop production represents the volume of water needed to sufficiently lower nitrogen concentrations that reach the water systems due to leaching or runoff, given an ambient NO_3^-N concentration of 10 mg l^{-1}, which corresponds to 44 mg l^{-1} of NO_3- (Self and Waskom, 2013, Shyns and Hoekstra, 2013). Increased N application rates beyond the optimal rate may significantly increase the *GWF*. On the other hand, a low N application rate can potentially hamper plant growth and result in a low crop yield (Raun et al., 2002) even though water pollution per hectare may still be small (Chukalla et al., 2017). Instead of carrying out laborious, time-consuming, and thus expensive field investigations with a limited number of treatments, an optimal N application rate can be estimated using a modeling approach (Karandish and Šimůnek, 2016a, 2016b, 2017). This may be especially advantageous in situations where it may be economically or technically impossible to carry out the project in the field (Li and Liu, 2011). Among a large number of analytical and numerical models simulating soil water and solute dynamics (e.g., Johnsson et al., 1987; Hutson and Wagenet, 1991; Ma et al., 2001; Šimůnek et al., 2008, 2016; Doltra and Munoz, 2010), the HYDRUS (2D/3D) model (Šimůnek et al., 2008, 2016) is among the most powerful models for evaluating sound agricultural practices due to its flexibility in accommodating different types of boundary conditions for water flow and solute transport, its ability to simultaneously consider root uptake of water and nutrients, and its sophisticated graphical user interface (Li et al., 2015; Karandish and Šimůnek, 2017).

The literature review reveals that there are many research gaps in this field of research. (i) Almost no research has been done on the use of the HYDRUS model to analyze soil-water-crop relationships under PRD. The concept behind PRD is different than behind DI and thus soil-water-crop relationships may be affected by these differences. While the HYDRUS model has been previously used to simulate soil water and nutrient dynamics under PRD (Karandish and Šimůnek, 2016a, 2016b, 2017), this has not yet been done while taking into account simultaneously both water and salinity stresses and their effects on soil-water-crop relationships. (ii) Similarly, little research has been carried out to find optimal management strategies with respect to both economic and environmental factors. While some limited work has been done with respect to finding an optimal combination of water-salinity-fertility levels for DI (Azizianand Sepaskhah, 2014a, 2014b), no similar work has been done for PRD. No research has considered simultaneously both environmental and economic indices when finding optimal management strategies for the DI or PRD strategies. (iii) Finally, no research has been carried out at the field scale to assess the total and grey water footprints under different combinations of water, fertility, and salinity stress (for both DI and PRD). While developing benchmark levels of the water footprint (*WF*) is still in its infancy, none of the previous studies have addressed the salinity stress in their analysis when benchmarking *WF*. In addition, the economic benefits associated with a more efficient water consumption due to benchmarking have not been quantified before.

Hence, the current study aims to advance the field of *WF* benchmarking by (i) developing field-specific benchmark levels for both total and grey *WFs* for various water-salinity-fertility scenarios and (ii) comparing the economic water productivities of the current crop production with productivities if *WFs* were reduced to benchmark levels. Therefore, the water footprint concept is applied in this study to provide the best 10% and 25% combinations of N-application rates and irrigation levels for different salinity rates under two water-saving irrigation strategies of DI and PRD with respect to both environmental and economic indices. The HYDRUS (2D/3D) model (its 2D level) is first calibrated and validated using a two-year field dataset and then used to analyze the soil-water-crop interactions for a large number of scenarios involving different combinations of N fertilizer rates, irrigation water levels, and salinity levels of the irrigation water under the DI and PRD conditions. The simulated results are then used (i) to calculate both consumptive and degradative *grey WF* related to crop production for various scenarios, (ii) to economically analyze the probable consequences of the defined scenarios, and, finally, (iii) to find the optimal management strategies with respect to both economic and environmental factors.

2. Materials and methods

2.1. Data collection

During the 2010 and 2011 cropping cycles, a two-year field investigation was carried out in the 825 m^2 (15 × 55 m) maize field at the Sari Agricultural Sciences and Natural Resources University in Sari, Iran. Daily weather data were collected at the weather station near the experimental field. Soil textures at 0–20 cm and 20–100 cm soil depths were sandy clay loam and clay loam, respectively. The randomized complete block design with five irrigation treatments (full irrigation [FI], two partial root-zone drying [PRD] treatments [PRD_{75} and PRD_{55}], and two deficit irrigation [DI] treatments [DI_{75} and DI_{55}]; the PRD and DI treatments were scheduled to receive 55% (PRD_{55} and DI_{55}) or 75% (PRD_{75} and DI_{75}) of the calculated irrigation volume of the FI treatment during each irrigation event) in three replicates was used in the field trial. The dimension of each treatment (i.e., the total land

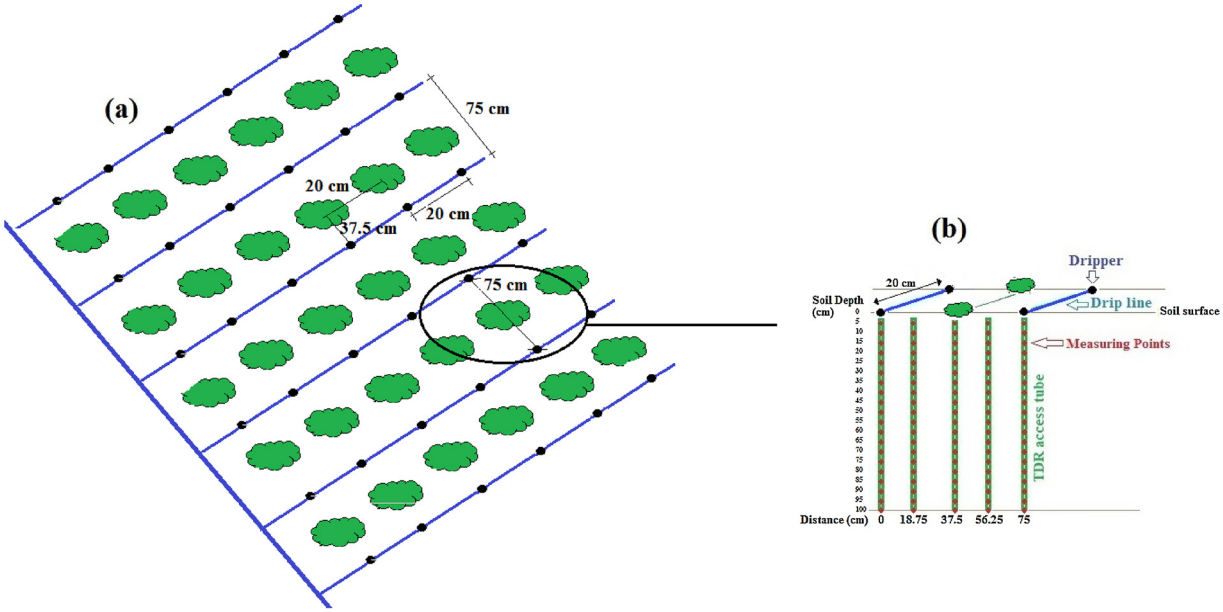

Fig. 1. Schematic of the field experimental site: the horizontal (a) and vertical (b) plans.

Table 1
Detailed description of field activities during the cropping cycles of 2010 and 2011.

No.	Activity	Description
1	Sowing	Maize single-cross hybrid 704 was sown 5 cm deep, with 75 cm × 20 cm crop row and crop spacings, respectively, between and parallel to the drip lines.
2	N fertilization	Urea was applied via irrigation (fertigation) with rates of 65 kg ha^{-1} and 135 kg ha^{-1} on July 14, 2010 and July 4, 2011, respectively.
3	P fertilization	150 kg ha^{-1} triple superphosphate was banded in crop rows prior to sowing date.
4	K fertilization	Potassium sulfate was applied via irrigation (fertigation) with rates of 50 kg ha^{-1} and 100 kg ha^{-1} on July 14, 2010 and July 4, 2011, respectively.
5	Irrigation treatments (ITs)	ITs included a full irrigation (FI) treatment, two partial root-zone drying (PRD) treatments (PRD_{75} and PRD_{55}), and two deficit irrigation (DI) treatments (DI_{75} and DI_{55})], each in three replicates, which were carried out in the randomized complete block design.
6	Stress periods	ITs were applied during 55-107 and 45-110 days after sowing (DAS) in 2010 and 2011, respectively.
7	Irrigation events	All treatments received the same amount of irrigation water during the first 55 and 45 DAS in 2010 and 2011, respectively. Different ITs were applied during 55-107 DAS in 2010 and 45-110 DAS in 2011. During this stress period, the PRD and DI treatments were scheduled to receive 55% (PRD_{55} and DI_{55}) or 75% (PRD_{75} and DI_{75}) of the calculated irrigation volume of the FI treatment (Eq. (1)) during each irrigation event. While in the DI treatments, the irrigation volume at each dripper was reduced by 25 or 45% (in DI_{75} and DI_{55}, respectively), in the PRD treatments one dripper line was alternatively not used at all, while the irrigation volume at the other dripper line was increased by 50 and 10% in PRD_{75} and PRD_{55}, respectively. The irrigated and non-irrigated sides were switched weekly in the PRD treatments.
8	Irrigation water sampling	Irrigation water quality was analyzed for all irrigation events.
9	Soil water content (SWC) measurements	TDR probes were used at least two times a day to measure SWCs in 5-cm depth increments during both growing seasons. Moreover, information about the movement of the wetting front during irrigation events was collected at least 10 times in each treatment by measuring SWCs one hour before, and immediately and 2, 6, 12, 24, 48, 72, and 96 hours after irrigation events in the 2010 growing seasons.
10	Soil sampling during cropping cycles	Prior to applying ITs, and once a week during the stress period, soil samples were collected in each treatment vertically every 20 cm to a depth of 80 cm and at five equal horizontal distances between two drip lines. Soil samples were analyzed for total nitrogen (TN) (the semi-micro Kjeldhal method (Bremner and Mulvaney, 1982)), the NO_3^--N concentration (with a spectrophotometer (DR/2500, Hack Co.) using a cadmium reduction method (APHA, 1992)), and the electrical conductivity (EC_{sw}).
11	Crop sampling during cropping cycles	At the same dates as soil sampling, three plants per plot (i.e., each plot is considered as one replicate of a treatment) were harvested to determine total crop N uptake, total wet and dry biomass, and leaf area index (LAI). Crop N uptake was determined using a semi-micro Kjeldahl apparatus. The oven-dried weight of crops at 70 °C was considered as the crop dry biomass. A laboratory leaf area meter (Delta-t Devices Ltd.) was used to measure the entire leaf area, which was converted to *LAI* by dividing it with the corresponding soil surface covered by the plants.
12	Soil and crop sampling at harvest	All considered soil and crop properties as well as maize grain yield were also determined at harvest.
13	Harvest	Crops were harvested on September 9, 2010 and September 12, 2011 (107 and 110 DAS, respectively).

allocated to three replicates of one treatment) was 165 m^2. The surface drip irrigation system was installed before sowing. Drip lines with emitters 20 cm apart and an emitter discharge rate of 2 L hr^{-1} were placed on the soil surface 75 cm apart (Fig. 1). Five 100 cm long TDR probes (Trime FM; IMKO; Germany) were then installed in each treatment as illustrated in Fig. 1 for continuous measurements of soil water contents (SWCs) (see Table 1). The accuracy of soil water contents measured using TDRs was compared with that measured using the gravimetric method. An index of agreement for these two methods was 95%, confirming the acceptability of TDR measurements.

After sowing, the experimental plots were irrigated every other day during both growing seasons. For the FI treatment, the net irrigation depth ($[I_n]_{FI}$, mm) was calculated as follows (Karandish and Šimůnek, 2016a, 2016b, 2017):

$$[I_n]_{FI} = \sum_{i=1}^{j} ((\theta_{FCi} - (\theta_{BIi})_{FI}) \times D_i) \quad (1)$$

where θ_{FCi} is the volumetric soil water content at field capacity (cm^3cm^{-3}) of the ith soil layer (field capacity for individual soil layers was determined prior to the field experiment), $(\theta_{BIi})_{FI}$ is the volumetric soil water content before irrigation in the ith soil layer (cm^3cm^{-3}) in the FI treatment, D_i is the soil layer thickness (mm), i is the soil layer counter, and j refers to the number of soil layers for which $[I_n]_{FI}$ is calculated. $(\theta_{BIi})_{FI}$ is the average SWC measured using TDR probes in different measuring points in the ith soil layer (Fig. 1). All plots received the same amount of irrigation water during the first 55 and 45 DAS in 2010 and 2011, respectively. Irrigation treatments were started on 55 and 45 DAS in 2010 and 2011, respectively. Additional information about field activities during the stress period (55–107 and 45–110 DAS in 2010 and 2011, respectively) can be found in Table 1. Detailed information can also be found in Karandish and Šimůnek (2016a, 2016b, 2017).

2.2. HYDRUS (2d/3d)

The HYDRUS (2D/3D) model (its 2D level) (Šimůnek et al., 2008, 2016) was used for simulating water, NO_3^-N, and EC dynamics in soil. In this model, water flow is described using the Richards equation (Eq. (2)) while the convection-dispersion equation (CDE) is used for the solute (electrical conductivity of the soil solution (EC_{sw}) and NO_3^-N) transport (Eq. 3):

$$\frac{\partial \theta}{\partial t} = \frac{\partial}{\partial x}\left(K_x \frac{\partial h}{\partial x}\right) + \frac{\partial}{\partial z}\left(K_z \frac{\partial h}{\partial z}\right) - \frac{\partial k}{\partial z} - WU(h, h_{\varnothing}, x, z) \quad (2)$$

$$\frac{\partial \theta c}{\partial t} = \left\{\frac{\partial}{\partial x}\left(\theta D_{xx} \frac{\partial c}{\partial x} + \theta D_{xz} \frac{\partial c}{\partial z}\right) + \frac{\partial}{\partial z}\left(\theta D_{zz} \frac{\partial c}{\partial z} + \theta D_{zx} \frac{\partial c}{\partial x}\right)\right\} - \left(\frac{\partial q_x c}{\partial x} + \frac{\partial q_z c}{\partial z}\right) - S_c \quad (3)$$

where Θ is the volumetric SWC (L^3L^{-3}), K is the unsaturated hydraulic conductivity function (LT^{-1}), h is the soil water pressure head (L), x is the lateral coordinate, z is the vertical coordinate (positive downwards), t is time (T), $WU(h, h_{\varnothing}, x, z)$ denotes root water uptake (T^{-1}), c is the solute concentration in the liquid phase (ML^{-3}), q_x and q_z are the components of the volumetric flux density (LT^{-1}), D_{xx}, D_{zz}, and D_{xz} are the components of the dispersion tensor (L^2T^{-1}), and S_c is the sink term (nutrient uptake, $ML^{-3}T^{-1}$).

The equation of Feddes et al. (1978) was used to determine the root water uptake sink term in Eq. (2):

$$WU(x, z, h, h_{\varnothing}) = \alpha(x, z, h, h_{\varnothing}) b(x, z) WT_p \quad (4)$$

where $\alpha(x, z, h, h_{\varnothing})$ is the soil water (h) and osmotic ($h_{\varnothing}$) stress response function (dimensionless), $b(x, z)$ is the normalized spatial root water uptake distribution (L^{-2}), W is the width of the soil surface associated with transpiration (L), and T_p is potential transpiration (LT^{-1}). A full description of how potential crop water requirements, potential evaporation (E_p), and potential transpiration (T_p) are calculated is described in Karandish and Šimůnek (2016a).

It is assumed that potential root water uptake is reduced due to the water stress when crops are supplied with an insufficient amount of irrigation water and due to the osmotic stress when crops are irrigated with saline water. Following van Genuchten (1987), the influence of water and salinity stresses were considered to be multiplicative (i.e., $\alpha(x, z, h, h_{\varnothing}) = \alpha(x, z, h)\alpha(x, z, h_{\varnothing})$, so that different stress response functions could be used for the water and salinity stresses (Ramos et al., 2012). Karandish and Šimůnek (2016a, 2016b, 2017) described the root water uptake reduction caused by the water stress ($\alpha(x, z, h)$) using the piecewise linear model proposed by Feddes et al. (1978). The salinity threshold (EC_T) and slope function (Mass, 1990) was used to simulate the root water uptake reduction due to the salinity stress. Using the HYDRUS (2D/3D) database of suggested crop-specific parameters for the solute stress (Šimůnek et al., 2011), the salinity threshold EC_T and slope for maize were set to 1.7 dS m^{-1} and 12%, respectively. Since EC_T denotes the electrical conductivity of the saturation extract (EC_e), this value was converted into EC_{sw}, which is required by HYDRUS (2D/3D). Following earlier recommendations (US Salinity Laboratory, 1954; Skaggs et al., 2006), it was assumed that $EC_{sw}/EC_e = 2$. Detailed information about how root water and nutrient uptake was simulated can be found in Karandish and Šimůnek (2016a, 2016b, 2017).

The rectangular two-dimensional transport domain (75 cm wide and 80 cm deep, i.e., the maximum observed rooting depth) was defined between two neighboring emitters on either side of one plant. Drip lines were considered to be line sources since the emitter spacing (20 cm) along the driplines was relatively small. The simulation domain was discretized with a non-uniform finite element mesh generated by the HYDRUS model with finite element sizes gradually increasing with distance from the emitters. Soil hydraulic properties, measured as described in Karandish and Šimůnek (2016a), were defined for two soil horizons of the 0–20 cm and 20–80 cm soil depths.

Within the flow domain, measured SWC, NO_3^--N, and EC_{sw} at the beginning of the experiment were used as initial conditions for simulations. The time-variable and atmospheric boundary conditions were specified at the soil surface to represent drip irrigation and to apply precipitation, evaporation, and transpiration fluxes, respectively. A free drainage boundary condition was applied along the bottom boundary, allowing for downward drainage. Both solute species (NO_3^--N and EC) were applied with irrigation water, and therefore a third-type Cauchy boundary condition was used to describe concentration fluxes along the surface boundary. All other remaining boundaries were assigned a no-flow boundary condition.

The HYDRUS model was calibrated and validated for the soil hydraulic and chemical properties using the two-year experimental data. An inverse solution option in the model was used to optimize the saturated hydraulic conductivity (K_s), the saturated soil water content (θ_s), and the residual soil water content (θ_r) as soil hydraulic properties, as well as the longitudinal (D_L, L) and transversal dispersivities (D_T, L) as soil solute transport properties. The initial value of D_L was set to one tenth of the soil depth, and the initial value of D_T was set to one tenth of D_L (Ramos et al., 2012). The molecular diffusion coefficient was always set to zero since molecular diffusion can usually be neglected (Radcliffe and Šimůnek, 2010). In the calibration process, the capability of HYDRUS was assessed by comparing the simulated and observed data (i.e., SWC, NO_3^-N, and EC_{sw}) during the 2010 growing season. Afterwards, the optimized soil hydraulic and solute transport parameters obtained by calibration were used to validate the model by comparing the simulated and observed data (SWC, NO_3–N, and EC_{sw}) during the 2011 growing season.

As discussed in our earlier publications, the effects of PRD may differ from DI due to its positive influence on the abscisic acid (ABA) secretion, which causes improved root hydraulic conductivity and secondary root initiations and, consequently, improved root water uptake and crop water productivity (Karandish and Šimůnek, 2016a). Hence, we attempted to address such differences between PRD and DI when calibrating HYDRUS-2D. In fact, the model was separately calibrated for full irrigation, DI, and PRD treatments since a comprehensive dataset was collected on temporal variations of root and shoot growth during both cropping cycles of 2010 and 2011. The horizontal and vertical root distributions at each sampling date were determined using the Auger Sampling method (Kumar et al., 1993). Roots were sampled with a 2-in ID auger every 10 cm down to a depth of 80 cm and horizontally every 10 cm between two drip lines. Feddes' parameters were adjusted for each water-saving irrigation strategy (DI or PRD), which led to a higher agreement between observed and simulated soil water balance components (Karandish and Šimůnek, 2016a, 2016b, 2017). Detailed information about the calibration and validation process and the soil hydraulic and solute transport parameters can be found in

Karandish and Šimůnek (2016ab, 2017).

2.3. Scenario assessment

After calibrating and validating the HYDRUS models, different management scenarios were defined to analyze the combined influence of the N-management, water-saving strategies, and irrigation water quality strategies on the economic and environmental measures in the study area. Various scenarios were defined using combinations of the ratio of the applied irrigation water depth to the full irrigation water depth (IL) (note that the full irrigation water depth was calculated based on Eq. (1), the N-fertilizer application rate (NR), and the salinity of irrigation water (SR). All scenarios were defined for two irrigation strategies of DI and PRD. IL was increased in 10% steps from 0 to 100% of the full irrigation water depth, NR in 50 kg ha^{-1} intervals from 0 to 400 kg ha^{-1}, and SR in 1 dS m^{-1} increments from 0 to 8 dS m^{-1}. HYDRUS was then run for all scenarios to estimate water and solute balance components. Using simulated crop N uptake, the yield equation of Karandish and Šimůnek (2017) was then applied to estimate crop yield for all scenarios:

$$Yield = 0.0311 \times (N\ uptake) + 1.0654 \quad (5)$$

where both crop *Yield* and *N uptake* (i.e., the seasonal amount of crop N uptake) are presented in kg ha^{-1}.

The water footprint (*WF*, m^{3}t^{-1}), introduced by Hoekstra (Hoekstra et al., 2011), is considered to be a multi-dimensional measure of the amount of freshwater that is used directly by the producer or indirectly by the consumer. The consumptive *WF* (m^{3}t^{-1}) of the crop production includes both green and blue components, which refer to rainfall and irrigation water, respectively. The consumptive *WF* is calculated as follows:

$$consumptive\ WF = \frac{ET}{Yield} \quad (6)$$

where *ET* is the actual crop water consumption (m^3 ha^{-1}) during the entire cropping cycle and *Yield* is crop yield (t ha^{-1}). The consumptive *WF* is different from the degradative grey WF, or the so-called grey *WF* (*GWF*), which represents the volume of water required to sufficiently dilute pollutants entering freshwater bodies. The *GWF*, which may be considered as an indicator of the pollution assimilation capacity (Chukalla et al., 2017), was calculated for the N fertilizer following the Global Water Footprint Standard (Hoekstra et al., 2011) as the volume of water per a ton of crop as follows:

$$GWF = \frac{\beta S}{(C_{max} - C_{nat})Y} \quad (7)$$

where β is the leaching-runoff fraction, S (kg ha^{-1} y^{-1}) is the amount of N applied but not taken up by plants, C_{max} and C_{nat} are the maximum acceptable and natural N concentrations (kg m^{-3}), respectively, and Y is the crop yield (t ha^{-1}y^{-1}). Based on values suggested in Franke et al. (2013), we set $\beta = 0.44$ for N. A maximum acceptable N concentration of 50 mg L^{-1} (or 11.3 mg L^{-1}) is adopted based on the EU Nitrates Directive (Monteny, 2001). The natural concentration of N was considered to be zero.

The economic analysis was carried out based on the economic water (*EWP*, $ m^{-3}) and land (*ELP*, $ ha^{-1}) productivity indices, calculated as follows (Aldaya et al., 2010):

$$EWP = \frac{P}{consumptive\ WF} \quad (8)$$

$$ELP = P^{*}Yield \quad (9)$$

where P is the producer price ($ ton^{-1}), which was set to 323.4 $ ton^{-1} according to the FAO statistics for Iran (FAO, 2015).

2.4. Statistical analysis

The root mean square error (*RMSE*), the mean bias error (*MBE*), and the model efficiency (*EF*) were calculated to provide a quantitative assessment of the correspondence between predicted and observed data as follows:

$$RMSE = \sqrt{\frac{\sum_{i=1}^{n}(O_i - P_i)^2}{n}} \quad (10)$$

$$MBE = \frac{\sum_{i=1}^{n}(O_i - P_i)}{n} \quad (11)$$

$$EF = 1 - \frac{\sum_{i=1}^{n}(O_i - P_i)^2}{\sum_{i=1}^{n}(O_i - \overline{O_i})^2} \quad (12)$$

where P_i and O_i are the predicted and observed data, respectively, n is the number of observations, and $\overline{O_i}$ is the average of observed data.

3. Results and discussion

3.1. The performance of the numerical model

Similarly as in other studies (e.g., Cote et al., 2003; Gärdenäs et al., 2005; Assouline et al., 2006; Hanson et al., 2006; Ajdary et al., 2007; Crevoisier et al., 2008; Siyal and Skaggs, 2009; Mubarak, 2009; Li and Liu, 2011; Ramos et al., 2012; Tafteh and Sepaskhah, 2012; Phogat et al., 2013), HYDRUS successfully simulated soil water and NO_3^--N dynamics in the study area (Karandish and Šimůnek, 2016a, 2016b, 2017). HYDRUS was further applied to simulate *EC* dynamics (Fig. 2) using the soil hydraulic and solute transport parameters optimized by Karandish and Šimůnek (2016a, 2016b, 2017) The agreement between observed and simulated soil EC_{sw} data during both growing seasons was, in addition to the visual inspection (Fig. 2), quantitatively assessed using the Root Mean Squared Error (*RMSE*) and the Mean Bias Error (*MBE*) statistics (Table 2). With respect to EC_{sw} concentrations, the *RMSE* ranged from 0.5 to 1.06 dS m^{-1} for the 0–20 cm soil depth, from 0.43 to 0.90 dS m^{-1} for the 20–40 cm soil depth, from 0.17 to 0.58 dS m^{-1} for the 40–60 cm soil depth, and from 0.14 to 0.53 dS m^{-1} for the 60–80 cm soil depth. While the *MBE* (0.09-0.92 dS m^{-1}) between observed and simulated EC_{sw} in different soil layers was relatively small, it was larger in the surface layer (MBE = 0.17-0.92), which can probably be attributed to higher changes in the EC_{sw} concentrations during the simulation process (Karandish and Šimůnek, 2016a,b).

Fig. 2 compares temporal variations of simulated and observed EC_{sw} concentrations in different soil layers for the FI treatment during the 2010 cropping cycle so as to illustrate the capability of HYDRUS of capturing the temporal trends of EC. Simulated *EC* concentrations agreed well with observed values, with the EF ranging from 0.88-0.99 and 0.91-0.97 in 2010 and 2011, respectively. A close match between simulated and observed EC_{sw} concentrations, as well as their seasonal trends, was also obtained in other studies for various soils and crops under pressurized irrigation conditions (e.g., Ramos et al., 2011 and 2012; Phogat et al., 2014; Zeng et al., 2014; Mguidiche et al., 2015). Hence, the results of the quantitative assessment reported in Table 2 and the visual inspection of the results displayed in Fig. 2 indicate that HYDRUS can be used to evaluate the hypothetical scenarios considered in this study and discussed below.

3.2. Analysis of evaluated scenarios

The results of HYDRUS simulations for evaluated scenarios are discussed in the following sections with respect to both environmental and economic factors, including the effects on the crop water consumption, crop N uptake, crop yield, the consumptive *WF*, the degradative grey *WF*, and the economic land and water productivity.

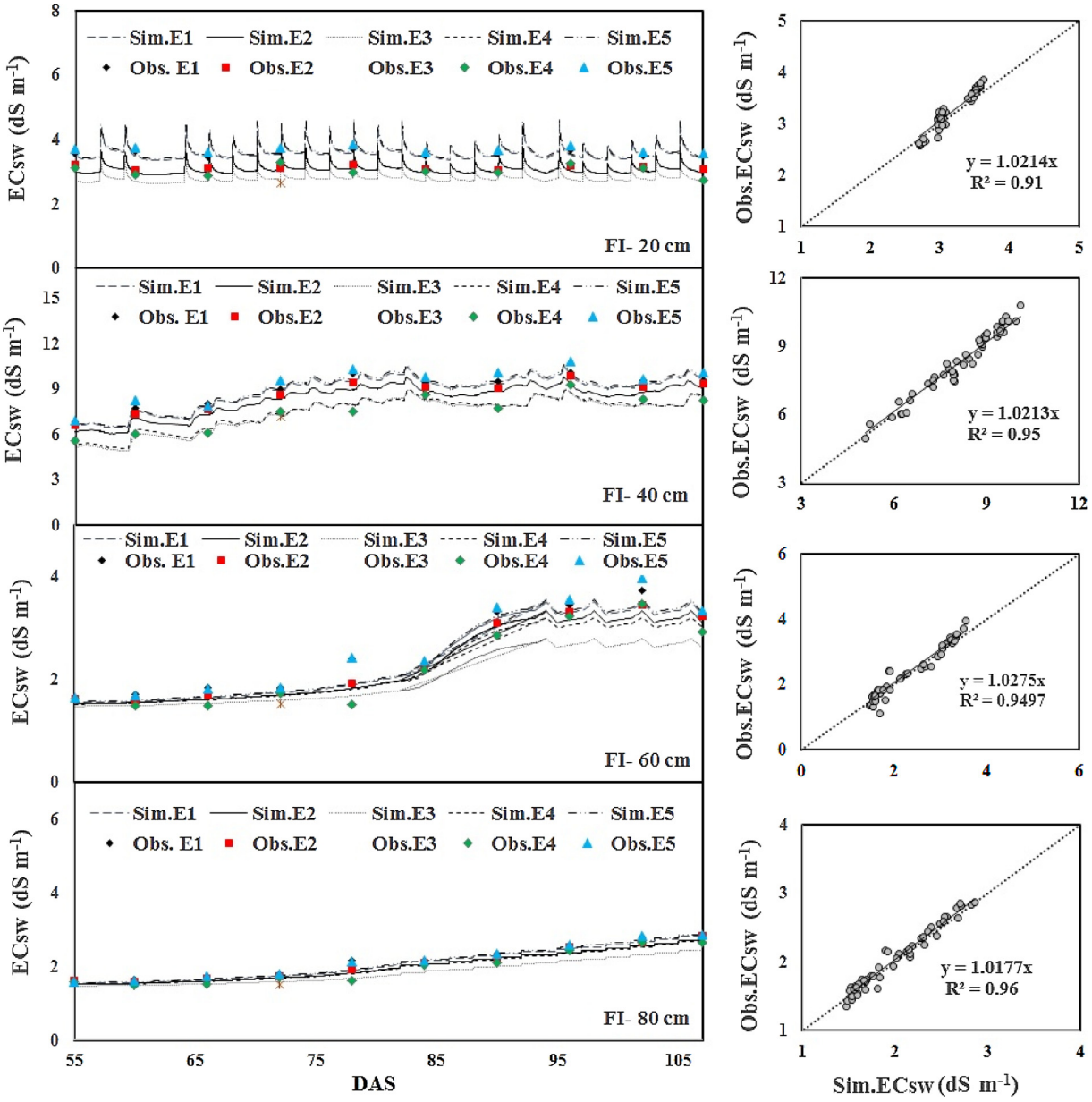

Fig. 2. Observed and simulated EC_{sw} at different depths (top to bottom: 0–20 cm, 20–40 cm, 40–60 cm, and 60–80 cm) during the 2010 growing season for the FI irrigation treatment at different horizontal locations. DAS is the number of days after sowing. E1, E2, E3, E4, and E5 refer to the lateral positions of EC measurements (i.e., the first dripper (Fig. 1), and 18.75, 37.5, 56.25, and 75 cm away from the first dripper, respectively).

Table 2
Model performance criteria (dS m^{-1}) at different soil depths for the 2010 and 2011 datasets. RMSE and MBE are the root mean squared and mean biased errors, respectively.

Year	depth (cm)	Treatment									
		FI		PRD75		PRD55		DI75		DI55	
		RMSE	MBE	RMSE	MBE	RMSE	MBE	RMSE	MBE	RMSE	MBE
2010	0-20	0.74	0.28	1.01	0.92	0.74	0.37	0.85	0.25	0.50	0.17
	20-40	0.63	0.23	0.85	0.74	0.56	0.28	0.66	0.21	0.44	0.15
	40-60	0.47	0.18	0.55	0.48	0.17	0.15	0.43	0.14	0.39	0.13
	60-80	0.36	0.13	0.34	0.30	0.14	0.12	0.39	0.13	0.27	0.09
2011	0-20	0.58	0.23	0.54	0.37	0.58	0.46	1.06	0.64	0.70	0.28
	20-40	0.49	0.19	0.43	0.30	0.43	0.34	0.90	0.54	0.61	0.24
	40-60	0.37	0.15	0.28	0.19	0.17	0.15	0.58	0.35	0.53	0.21
	60-80	0.28	0.11	0.17	0.12	0.14	0.12	0.53	0.32	0.37	0.15

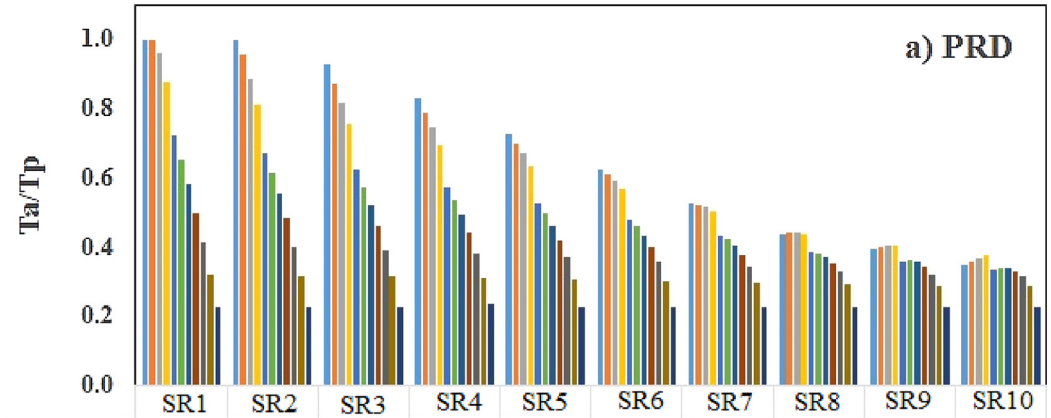

	SR1	SR2	SR3	SR4	SR5	SR6	SR7	SR8	SR9	SR10
IL=100%	1.00	1.00	0.93	0.83	0.73	0.63	0.53	0.44	0.39	0.35
IL=90%	1.00	0.96	0.87	0.79	0.70	0.61	0.52	0.44	0.40	0.36
IL=80%	0.96	0.89	0.82	0.74	0.67	0.59	0.51	0.44	0.40	0.37
IL=70%	0.87	0.81	0.75	0.69	0.63	0.57	0.50	0.44	0.41	0.37
IL=60%	0.72	0.67	0.62	0.58	0.53	0.48	0.43	0.38	0.36	0.34
IL=50%	0.65	0.61	0.57	0.54	0.50	0.46	0.42	0.38	0.36	0.34
IL=40%	0.58	0.55	0.52	0.49	0.46	0.43	0.40	0.37	0.36	0.34
IL=30%	0.50	0.48	0.46	0.44	0.42	0.40	0.38	0.35	0.34	0.33
IL=20%	0.41	0.40	0.39	0.38	0.37	0.36	0.35	0.33	0.32	0.31
IL=10%	0.32	0.32	0.31	0.31	0.31	0.30	0.30	0.29	0.29	0.29
IL=0%	0.22	0.22	0.22	0.24	0.22	0.22	0.22	0.22	0.22	0.22

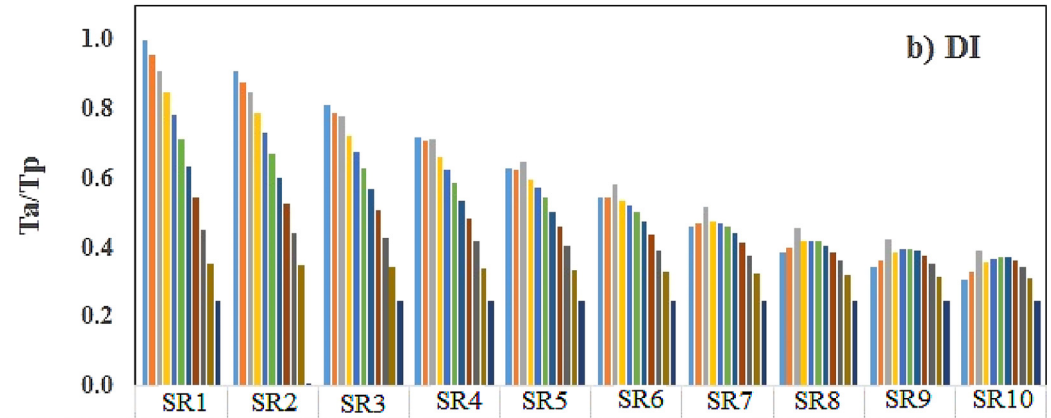

	SR1	SR2	SR3	SR4	SR5	SR6	SR7	SR8	SR9	SR10
IL=100%	1.00	0.91	0.81	0.72	0.63	0.54	0.46	0.38	0.35	0.31
IL=90%	0.96	0.88	0.79	0.71	0.62	0.55	0.47	0.40	0.36	0.33
IL=80%	0.91	0.85	0.78	0.71	0.65	0.58	0.52	0.45	0.42	0.39
IL=70%	0.85	0.79	0.72	0.66	0.60	0.54	0.48	0.42	0.39	0.36
IL=60%	0.78	0.73	0.68	0.63	0.57	0.52	0.47	0.42	0.39	0.37
IL=50%	0.71	0.67	0.63	0.59	0.54	0.50	0.46	0.42	0.39	0.37
IL=40%	0.63	0.60	0.57	0.54	0.50	0.47	0.44	0.41	0.39	0.37
IL=30%	0.54	0.53	0.51	0.48	0.46	0.44	0.41	0.39	0.37	0.36
IL=20%	0.45	0.44	0.43	0.42	0.41	0.39	0.38	0.36	0.35	0.34
IL=10%	0.35	0.35	0.34	0.34	0.33	0.33	0.32	0.32	0.32	0.31
IL=0%	0.25	0.00	0.25	0.25	0.25	0.25	0.25	0.25	0.25	0.25

Fig. 3. The ratio of actual (T_a) and potential (T_p) transpiration for various combinations of irrigation levels (IL: from 100% [the first column] to 0% [the last column] in 10% increments) and irrigation salinities (SR: SR1 through SR10) under PRD (a) and DI (b) irrigation strategies.

3.2.1. WF components

As introduced by Hoekstra (2002), *WF* (consumptive and degradative) is highly dependent on several components, which include crop yield, crop water consumption, and solute residual in soil. As mentioned by Chukalla et al. (2017), developing benchmark levels for various field practice scenarios requires a deep knowledge on their effects on WF components. Hence, here we first discussed the probable effects of various scenarios on the consumptive and degradative WF components and then, discussed their direct effects on consumptive and degradative WF.

3.2.1.1. Blue and green water consumption. Fig. 3 displays the ratio of actual (T_a) to potential (T_p) crop transpiration for various combinations of ILs and SRs. Regardless of the irrigation strategy (DI or PRD), the T_a/T_p ratio tends to progressively decrease in response to the salinity increase while only a minor variation in T_a/T_p was found when a high salinity stress was imposed (i.e., $7 \leq$ SR (dS m^{-1}) ≤ 10). Moreover, a higher T_a/T_p ratio for $40\% \leq$ IL $\leq 70\%$ and SR ≥ 7 dS m^{-1} indicates that imposing a mild water stress may improve root water uptake when crops are under a high salinity stress. Such results may be attributed to the reduced salt loaded into the rooting zone under deficit irrigation with highly saline water (Yazdani et al., 2004). The low T_a/T_p variation in response to a salinity increase under a high water stress also demonstrates the higher influence of the matric potential on the reduction in root water uptake compared to the osmotic stress, which was also confirmed by Kaya et al. (2015).

Reductions in root water uptake due to water and salinity stresses were a function of the adopted irrigation strategy. For $70\% \leq$ IL $\leq 100\%$, the T_a/T_p ratio under PRD was up to 15.5% higher than under DI, while for IL $\leq$ 60%, water and salinity stresses caused a 3.7–8.8% lower reduction in the T_a/T_p ratio under DI than under PRD. Earlier research demonstrated that the root system could partially compensate for the increasingly limited availability of water at the dry side of the row when crops are under PRD with a low to mild water stress (Kang et al., 2002; Liu et al., 2006; Sepaskhah and Ahmadi, 2010). Nevertheless, the rate of water supply was reported to be a prominent factor for sustaining the positive effects of PRD (Liu et al., 2006; Karandish and Shahnazari, 2016; Karandish and Šimůnek, 2016a, 2016b, 2017). Karandish and Šimůnek (2016a) reported favorable crop evapotranspiration under PRD with a 25% reduction in the irrigation demand (PRD_{75}) compared to DI_{75}, while DI led to higher root water uptake when the irrigation demand was reduced by 45% (DI_{55}) compared to PRD_{55}.

3.2.1.2. N uptake and yield. Crop N uptake (NU) was affected by ILs, NRs, and SRs (Fig. 4). While higher NU was achieved in the scenarios with lower SRs and higher NRs and ILs, the pattern of the increase was different among various scenarios. For all ILs and SRs, NU increased considerably (by 1–235%) when NR increased from 0 to 200 kg ha^{-1} and only slightly (0.3–10%) when it increased from 200 to 250 kg ha^{-1}. A considerable reduction in the NU upward slope for NR $\geq$ 250 kg ha^{-1} may lead to considerable environmental deterioration since the imbalance between N supply and N demand leaves more N in the soil after harvest, which may be subsequently leached out of the rooting zone as a result of off season precipitation (Karandish et al., 2016). Fig. 4 also shows that the range of NU variations is limited when crops are irrigated with brackish water with high salinity, resulting in a high water deficit stress.

PRD seems to be a more viable agro-hydrological option for reducing a pollutant load into groundwater since it led to higher NU and, consequently, lower N left in the soil after the harvest. Regardless of NRs, NU under PRD was 2.7–17.3%, 0.7–3.4%, and 0.2–1.3% higher than under DI for low (IL = 20%), moderate (IL = 50%), and high (IL = 80%) water stress conditions, respectively. This difference was more obvious for low to moderate salinity stresses while NU was slightly higher under PRD than under DI under the high osmotic stress

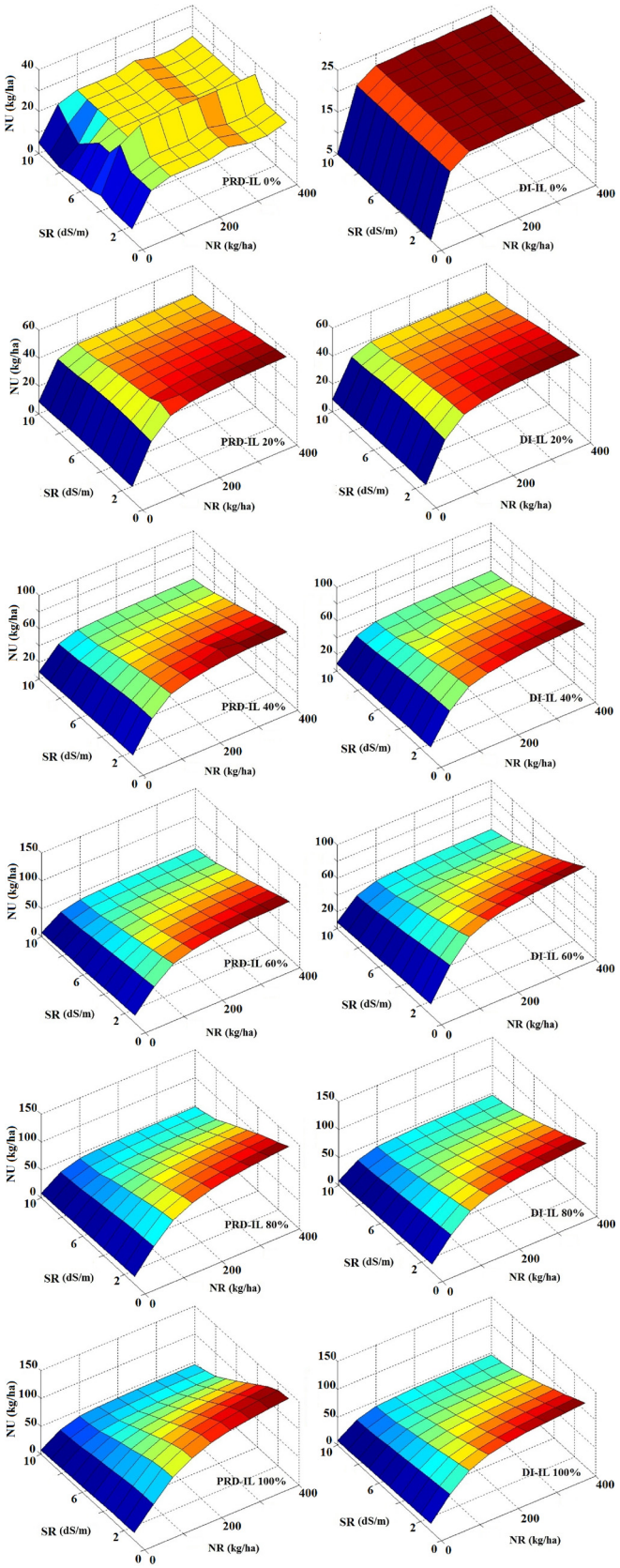

Fig. 4. Crop N uptake (NU; kg/ha) for various combinations of N fertilizations (NR, kg/ha), salinity rates (SR, dS/cm), irrigation levels (IL; %; from 0% [top] to 100% [bottom]), and irrigation (PRD - left, DI - right) strategies.

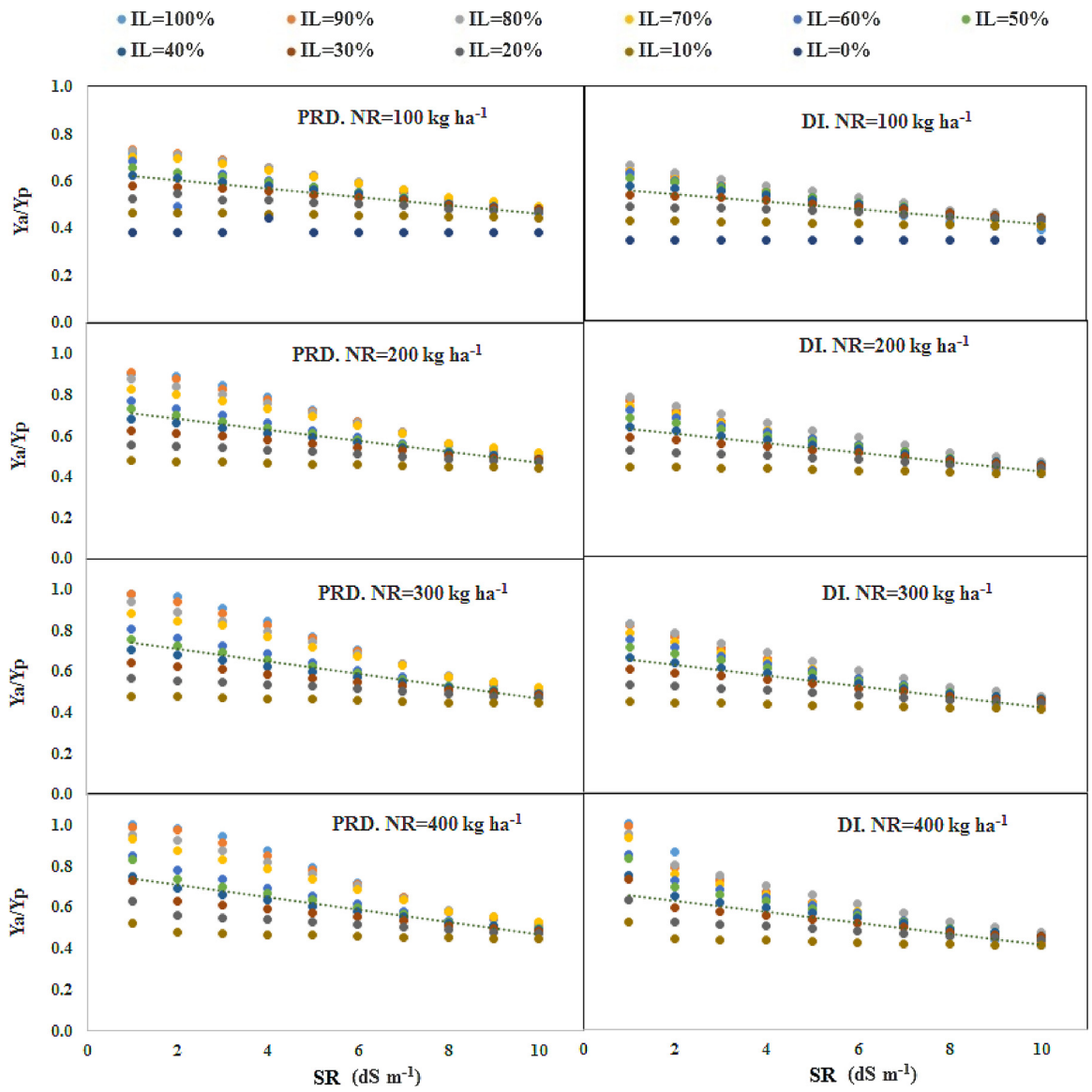

Fig. 5. The relation between relative maize grain yield (Y_a/Y_p) and salinity stress rates (SR) under various fertilization rates (NR, kg ha^{-1}, from 100 kg ha^{-1} [top] to 400 kg ha^{-1} [bottom]) and irrigation levels (IL) for the PRD (left) and DI (right) irrigation strategies.

(SR ≥ 7 dS m^{-1}), accounting for 3–6.6%, 0.7–1.1%, and 0.2-0.3% for low, moderate, and high water stress conditions, respectively. A substantially better performance of PRD may be attributed to the higher availability of N in the rooting zone, which may be caused by the frequent wetting and drying cycles (Nourbakhsh and Karimian Eghbal, 1997; Vale et al., 2007; Wang et al., 2010) or by the improved root growth and the extension of the root zone to deeper soil layers (Fort et al., 1997; Sepaskhah and Kamgar-Haghighi, 1997; Liang et al., 1996; Poni et al., 1992).

Fig. 5 relates the relative yield (Y_a/Y_p) to the salinity rate under various NRs and ILs. Although Y_a/Y_p decreased in response to any increase in the salinity stress, the pronounced Y_a/Y_p reduction (0.6–14% for PRD and 0.6–55% for DI) occurred when *SR* increased from 5 to 8 dS m^{-1}. A low to mild water stress under 5 ≤ SR ≤ 8 dS m^{-1} may enhance the downward slope of Y_a/Y_p to a greater extent. Nevertheless, the amount of irrigation water could be more profitably reduced when the high salinity stress is imposed. When 8 < SR ≤ 10 dS m^{-1}, Y_a/Y_p ranges from 0.38 to 0.58 under PRD and from 0.28 to 0.52 under DI, while Y_a/Y_p varied between 0.41–1 under PRD and between 0.29–1 under DI when 0 < SR ≤ 8 dS m^{-1}.

The negative influence of irrigation with saline waters on maize grain yield may be moderated under PRD since it led to 0.6–188% higher yield compared to DI for various scenarios. Such results may be particularly interesting when SR ≤ 4 dS m^{-1}, while significant improvements may not be observed when PRD crops are irrigated with highly saline water. In addition, maize grain yields are considerably higher (by 0.6–30.4%) under PRD than under DI for all NRs and SRs when IL ≥ 70%, while no considerable difference was observed in PRD or DI yields for IL ≤ 60%. Previous research also demonstrated higher yields under PRD compared to DI for non-saline conditions (Dry and Loveys, 1998); Kang and Zhang, 2004; Kirda et al., 2004; Tang et al., 2005; Shao et al., 2008; Wang et al., 2012; Karandish, 2016; Karandish and Šimůnek, 2016a), mainly due to better N nutrition and subsequent higher duration of vegetation growth (Haverkort et al., 2003) and a greater photosynthesis rate (Varvel et al., 1997; Gianquinto et al., 2003). The results of our previous research also demonstrated a significant influence of crop N nutrition on maize grain yield under PRD (Karandish and Šimůnek, 2017).

3.2.2. Consumptive and degradative grey WF

Fig. 6 shows the consumptive *WF*s of the crop production for different scenarios. When crops are fully irrigated (IL = 100%) with fresh

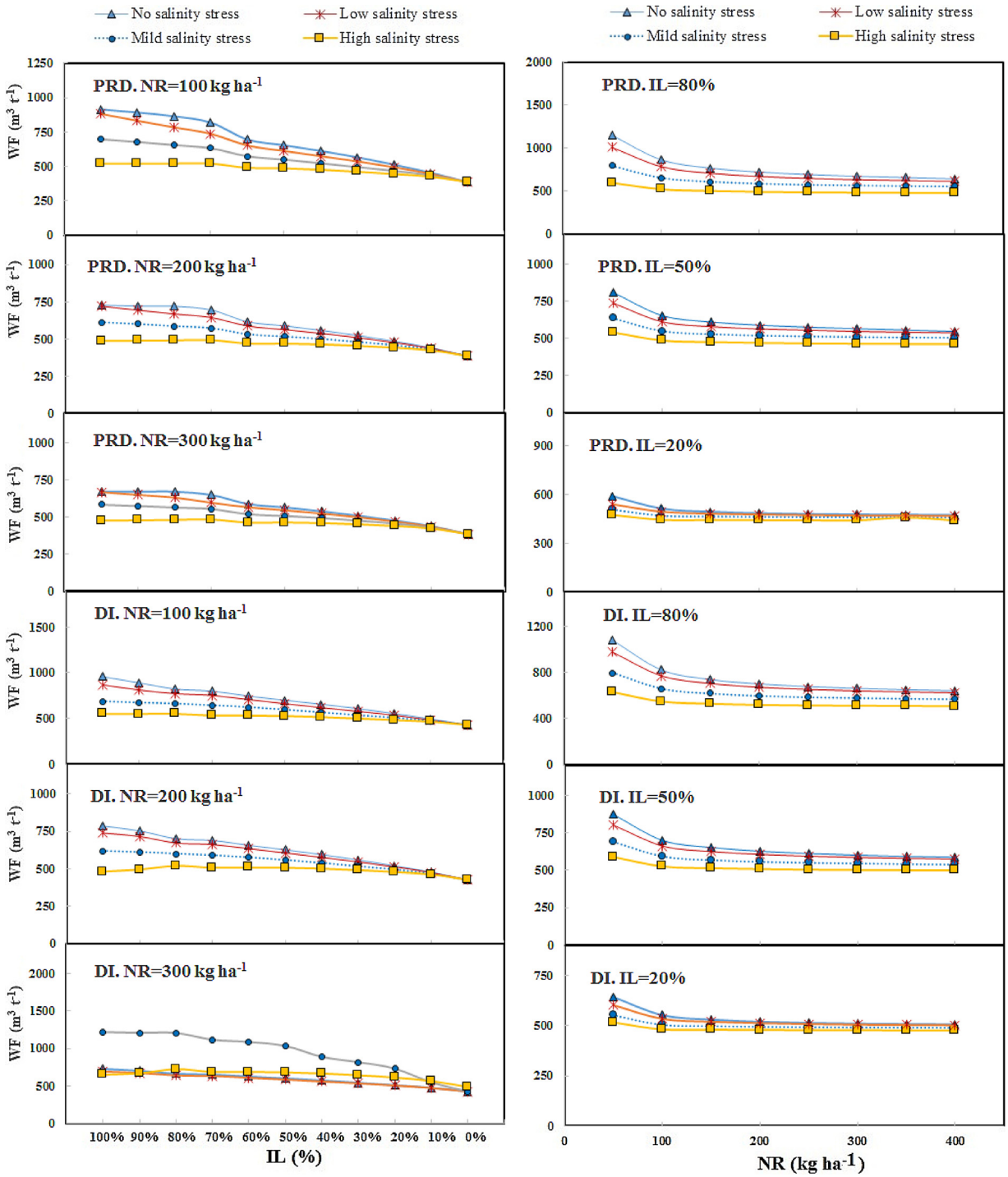

Fig. 6. The consumptive *WF* ($m^3 t^{-1}$) related to the crop production for various PRD (top) and DI (down) irrigation scenarios. IL (%; 80, 50, 20%) is the irrigation level and NR (kg ha^{-1}; 00, 200, 300 kg ha^{-1}) is the N-application rate.

water (SR = 1 dS m^{-1}), consumptive *WF*s vary within the range of 656-1985 $m^3 t^{-1}$ for PRD and 698-2080 $m^3 t^{-1}$ for DI, with higher values for lower NRs. At a given NR, the consumptive *WF* is reduced by 0.08–15.1% under PRD and by 0.1–25.1% under DI when the water deficit is induced. Moreover, a reduction of 0.8–25.5% and 0.6–47.0% is obtained under PRD and DI, respectively, when crops are exposed to the salt stress. The consumptive *WF*, which is defined as *ET* divided by yield, takes into account both crop yield and the crop water demand. While an increase in yield or a reduction in *ET* may directly increase the consumptive *WF*, any changes in the driving factors of yield and *ET* may affect the consumptive *WF* indirectly. Crop yield is a result of interactions between plant genetic traits, soil properties, field management, and climatic conditions (Karandish et al., 2014). Among these, field management is reported to be of the highest importance (Chukalla et al., 2015). This may explain different amounts of produced yield with a unit volume of consumed water in various scenarios.

For all combinations of ILs and SRs, the N application rates of 0-200 kg ha^{-1} caused a considerable reduction (up to 63%) in the consumptive *WF* due to a significant yield improvement (Fig. 5), while a less significant reduction (up to 17%) in the consumptive *WF* was observed when NRs increased above 200 kg ha^{-1}, likely due to the stabilized yield at large N application rates (Fig. 5). Furthermore,

improved N uptake under PRD aggravated the positive influence of an increased N application rate within the range of 0-200 kg ha^{-1} on the consumptive *WF* compared to DI. When NR = 200 kg ha^{-1}, an increased salinity stress reduced the consumptive *WF* at an average rate of 2.1 (for IL = 10%) to 34.2 (for IL = 100%) m^3 t^{-1} per a unit *EC* increase under PRD and at an average rate of 2 (for IL = 10%) to 40 (for IL = 100%) m^3 t^{-1} per a unit *EC* increase under DI. These findings result from a considerable reduction in the crop water consumption under the salt stress. Although the *ET* reduction may be converted into the yield reduction (Payero et al., 2006; Klocke et al., 2004; Stone, 2003), the consumptive *WF* may grow with a declining slope under increasing osmotic and matric water stresses when the rate of the ET reduction is far above the corresponding yield reduction.

With the absence of the salt stress, consumptive *WF* values may remain at their maxima when a low water stress is imposed (IL ≥ 70%) because of the higher crop water consumption. An intermediate to high water stress (IL < 70%) at SR = 1 dS m^{-1} may result in a quick reduction in the consumptive *WF* as a consequence of a pronounced decline in *ET* under low water availability conditions. When crops are under a low to intermediate salt stress, an increased matric water stress results in a steep linear reduction in the consumptive *WF*. The consumptive *WF*, however, exponentially decreases with IL when crops are exposed to the high saline stress (SR > 8 dS m^{-1}).

Fig. 7 presents the degradative grey *WF* (*GWF*) for various evaluated scenarios. The *GWF* linearly responds to an increase in the N application rate or salinity. The smallest *GWF* can always be found for an N application rate of zero or 50 kg ha^{-1}, where yield is very low (recall that yield is linearly related to N uptake). However, an increase in yield under higher N application rates comes at a price of a larger *GWF* due to higher amounts of N left in the soil after harvest. In the absence of salt or water stresses, the *GWF* may increase at average rates of 0.23 and 0.31 m^3 t^{-1} per a unit NR increase for PRD and DI, respectively. When crops are fully irrigated, inducing a salt stress may enhance the negative effect of large N application rates by increasing the *GWF* at an average rate of 0.1-1.8 m^3 t^{-1} per a unit *EC*. This increasing rate may be much higher when the irrigation water deficit is also integrated into the salt stress.

While higher *GWF*s were found for larger water deficits, an increasing trend in the *GWF* as a consequence of a lower soil water availability did not follow a linear equation. At NR = 200 kg ha^{-1}, which seems to be an optimal NR with regards to both economic and environmental issues, inducing a water stress of up to 30% (IL ≥ 70%) while crops are under a low to intermediate salt stress (SR ≤ 6 dS m^{-1}) results in a small increase in the *GWF* compared to full irrigation. The *GWF* also increases when IL*s* < 70%, but with a slope 1.8–54 times steeper. Nevertheless, *GWF*s tend to keep an increasing trend against an increase in the water stress when crops are under high salt stress (SR ≥ 6 dS m^{-1}).

3.2.3. Economic land and water productivity

Farmers may not adopt a new technology unless they are convinced that they can achieve an adequate economic return (Paredes et al., 2014; Karandish, 2016). Hence, we incorporated the accounted WFs into economic issue to calculate the economic water productivity (*EWP*, \$ m^{-3}) for various scenarios. The results are presented in Fig. 8. Under full irrigation with fresh water, the maize production yielded economic values of 0.16-0.50 \$ m^{-3}. Here, *EWP*s were 0.35, 0.44, 0.48, and 0.50 \$ m^{-3} for NR = 100, 200, 300, and 400 kg ha^{-1}, respectively, indicating that an increase in the N application rate above 200 kg ha^{-1} does not significantly improve the state of farm economics. Similar results were found for other combinations of IL and SRs. When a low water stress is imposed (70% ≤ IL ≤ 100%), the *EWP* increases non-linearly in response to an increase in SR for all NRs, with a steeper upward slope when 5 ≤ SR ≤ 10 dS m^{-1}. When IL > 70%, the rising trend of the *EWP* tends to follow a linear equation with R^2 = 0.85-0.98. Such results demonstrate the enormous potential for sustaining farm economics under higher water deficits and salinity stresses, which may be attributed to the fact that under such conditions, the T_a reduction is likely to be considerably higher compared to the corresponding yield reduction. Fig. 4 also shows that for all scenarios, applied water in the PRD scenarios yielded 0.1–163.9% more economic values compared to the DI scenarios.

While the *EWP* is an economic measure from the water viewpoint, the economic land productivity (*ELP*, \$/ha) may be more interesting for farmers since it represents the economic value of the farm output per hectare of the cultivated land. *ELP* values for various scenarios are illustrated in Fig. 9. Maize *ELP*s varied in the range of 463–1802 \$ ha^{-1} and 395–1785 \$ ha^{-1} for the PRD and DI scenarios, respectively. While the *ELP* increased considerably when NRs increased from 0 to 200 kg ha^{-1} (29–238% and 4–244% under the PRD and DI scenarios, respectively), only a slight increase in the *ELP* of 0.1–13.1% occurred for an additional increase in NRs above 200 kg ha^{-1}. When NR = 250 kg ha^{-1}, the *ELP* decreased considerably by 0.6–9.7% per a unit *EC* increase, except for non-irrigated crops, for which the *ELP* remained unchanged in response to the salinity increase. The *ELP* is non-linearly related to IL*s* for all combinations of NRs and SRs, indicating that the water stress induced at low rates (0 ≤ IL ≤ 70%) may lead to a more economically beneficial land use.

To find the optimal scenarios for NR = 200 kg ha^{-1} (i.e., the most beneficial threshold) from the viewpoint of both land and water economic returns, dimensionless *EWP* (dl.*EWP*) and *ELP* (dl.*ELP*) curves were plotted together against SRs or IL*s* in Fig. 10. The dimensionless *EWP* and *ELP* were calculated by dividing the absolute *EWP* or *ELP* values by the maximum *EWP* or *ELP* across the whole range of SRs and IL*s* at a given NR of 200 kg ha^{-1}. Fig. 10 shows that for PRD, different combinations of 60% ≤ IL ≤ 80% and 1 ≤ SR (dS m^{-1}) ≤ 4 may sustain both land and water economics, while optimal results for DI may be achieved only when a lower degree of the water stress 70% ≤ IL ≤ 90% is imposed on plants.

3.2.4. Benchmarking WFs

To develop benchmark levels for the consumptive and degradative WF within the study area, we need to find the optimal agricultural management practices. To find the optimal scenarios for a given SR, we first classified the evaluated measures into two groups: environmental measures including the apparent N-recovery efficiency (*ARE*) and the *GWF*, and economic measures including the *EWP* and the *ELP*. Following Mosier et al. (2004), the *ARE* was calculated by dividing crop N-uptake (kg ha^{-1}) by the N application rate (kg ha^{-1}). Four selected indices (*ARE*, *GWF*, *EWP*, and *ELP*) were first sorted from the worst to the best, and then they were scored. For each index, the highest score was considered to be the best value. Finally, the total score (*TS*) for each scenario (i.e., *TS* is the sum of the scores of the indices) was calculated, and then the optimal scenarios were determined based on the 10% and 25% highest *TS*s.

While there is an inevitable need for adjusting irrigation water and N-application rates when crops are irrigated with saline water, the results in Table 3 confirm that there is not one optimal combination of management practices when both environmental and economic issues are considered. In fact, the best management scenario highly depends on what variable is optimized (Chukalla et al., 2017). While high N-fertilization rates applied without water and salt stresses may yield higher economic returns, such scenarios may cause environmental deterioration due to the low *ARE* and high *GWF*. On the other hand, the optimal *ARE* and *GWF* may be achieved when less N is applied under moderate water and salt stresses. Hence, we developed WF benchmark levels through suggesting a range of optimal values for NRs and IL*s* at a given SR instead of proposing a single optimal management scenario.

Table 3 shows the optimal agricultural practices by which the benchmark levels for both consumptive and degradative grey WFs will be achieved within the study area. Regardless of the irrigation strategy (PRD or DI), both IL and NR need to be considerably reduced when

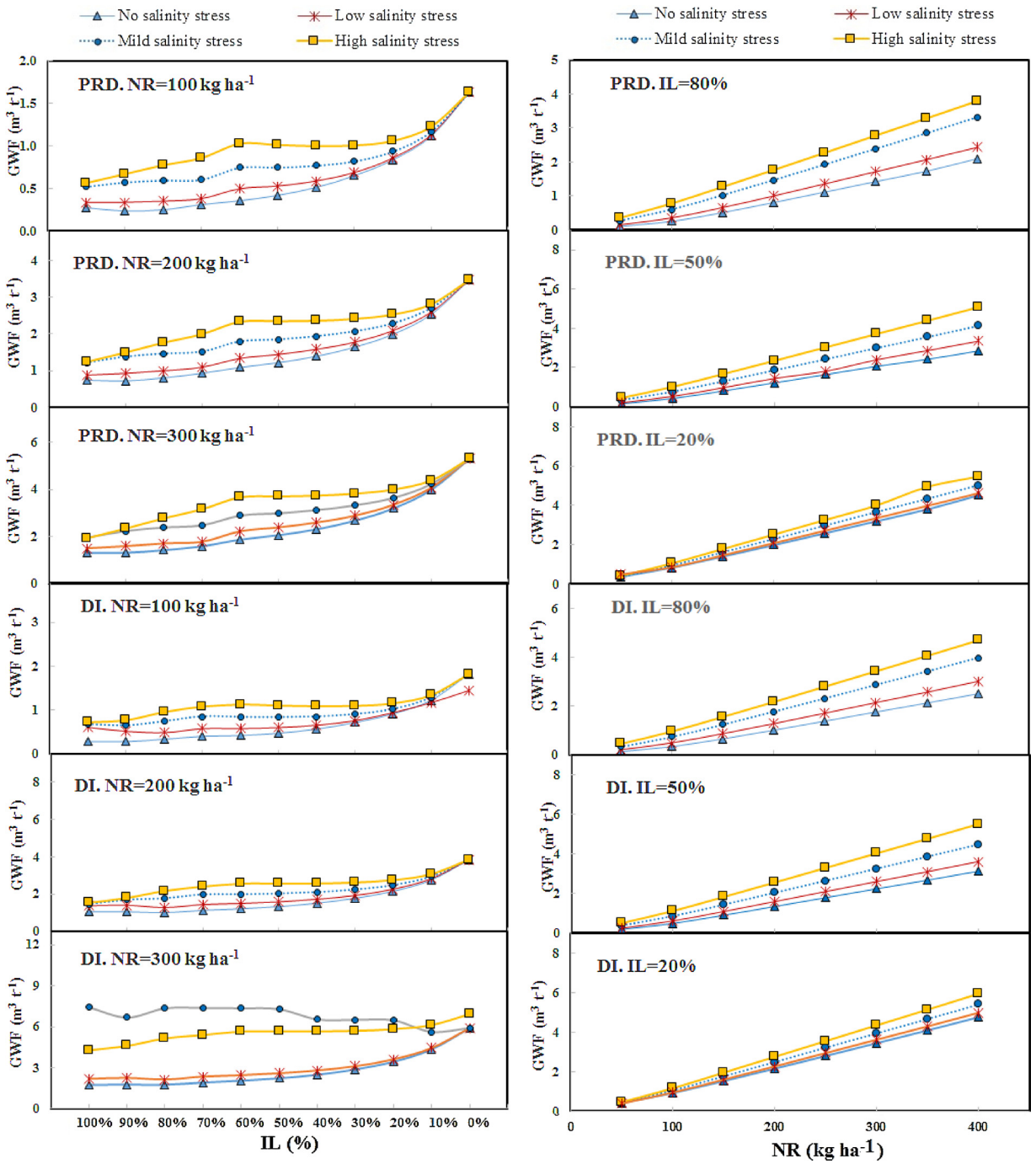

Fig. 7. The degradative grey *WF* (*GWF*; $m^3 t^{-1}$) related to the crop production for various PRD (top) and DI (down) scenarios. IL (%; 80, 50, 20%) is the irrigation level and NR (kg ha^{-1}; 00, 200, 300 kg ha^{-1}) is the N-application rate.

crops are irrigated with moderately or highly saline waters (SR > 5 dS m^{-1}) while a moderate adjustment may be required when crops are exposed to a milder salt stress (SR ≤ 5 dS m^{-1}). Besides, higher N-application rates and irrigation levels may be required when DI is applied compared to PRD, which in turn results from lower yield and water productivity under DI (Dry and Loveys, 1998); Kang and Zhang, 2004; Kirda et al., 2004; Tang et al., 2005; Shao et al., 2008; Wang et al., 2012; Karandish, 2016; Karandish and Šimůnek, 2016a). The analysis of obtained results (the evaluation indices) for evaluated scenarios indicates that the N-fertilization rates of 100-200 kg ha^{-1} applied at a mild salinity stress (SR < 5 dS m^{-1}) and the irrigation levels of 60–90% under the PRD irrigation strategy may be the best management scenarios.

4. Conclusions

The subject of establishing sound agricultural practices in the arid and semi-arid regions of the world presents many challenges, mainly related to water scarcity which may require the use of low-quality water and lead to subsequent environmental hazards. Hence, we conducted the first explorative study based on the concept of the water footprint to find out the optimal combination of N application rates and water application levels when crops are irrigated with saline water. The results simulated using HYDRUS (2D/3D) revealed that an increase in both yield and crop N uptake would level off at NR > 200 kg ha^{-1}. This is contrary to the viewpoint of many farmers who believe that higher economic returns are achieved by higher NR. Additionally, N

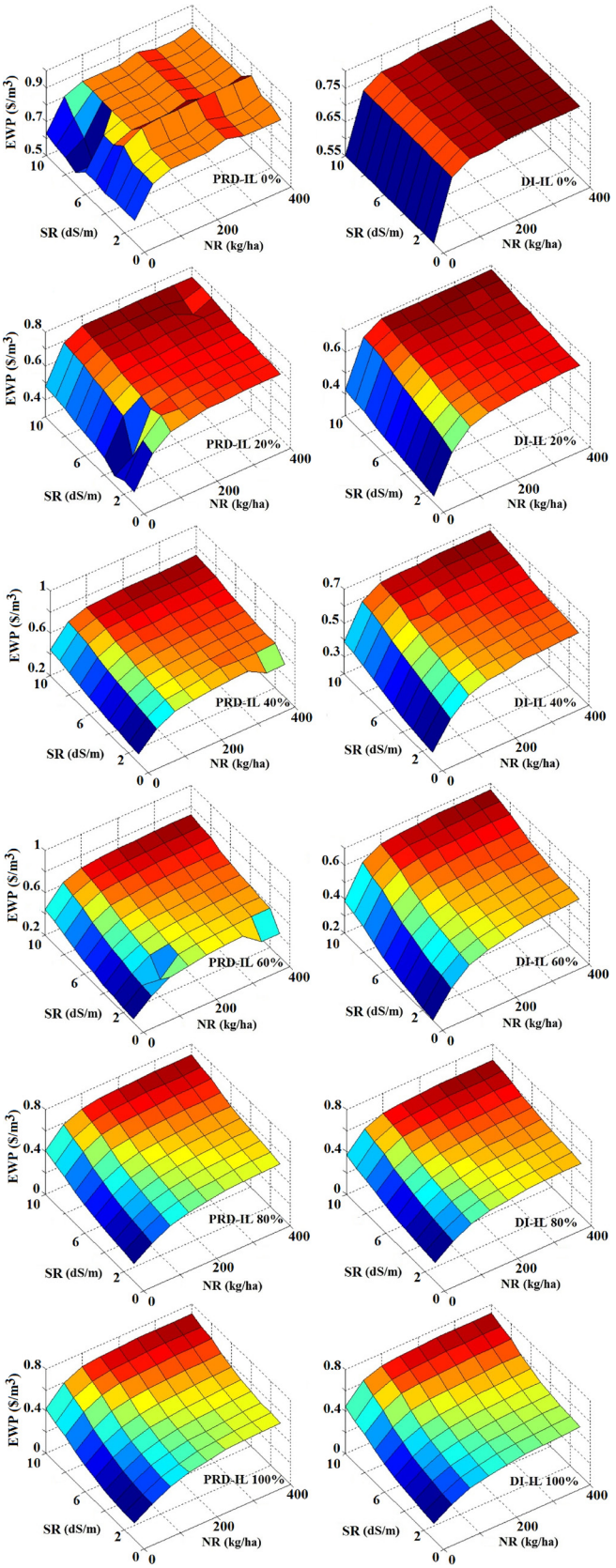

Fig. 8. The economic water productivity (EWP, $/m^3) for various combinations of N fertilizations (NR, kg ha^{-1}), salinity rates (SR, dS/cm), irrigation levels (IL, %), and irrigation (PRD – left, DI - right) strategies.

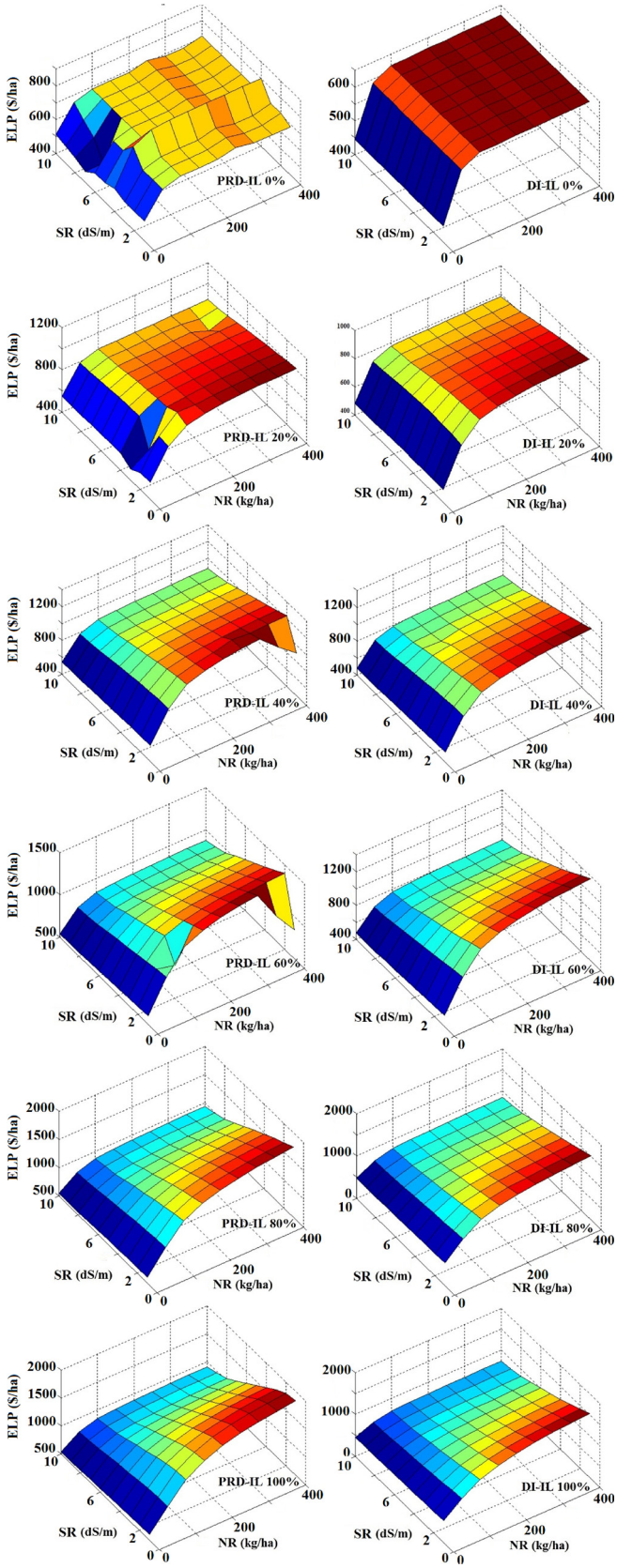

Fig. 9. The economic land productivity (*ELP*, $/ha) for various combinations of N fertilizations (NR, kg ha^{-1}), salinity rates (SR, dS/cm), irrigation levels (IL, %), and irrigation (PRD – left, DI - right) strategies.

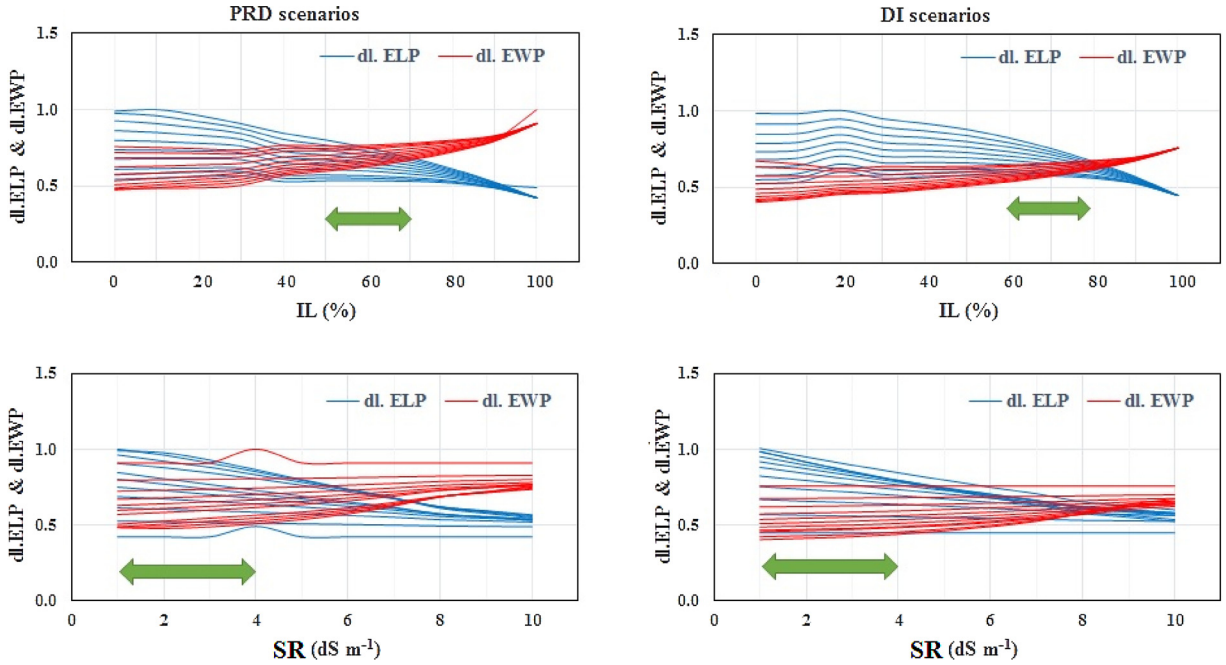

Fig. 10. Dimensionless *ELP* (dl. *ELP*) and *EWP* (dl. *EWP*) for the PRD (left) and DI (right) irrigation strategies for various water deficits (IL, %) (top) and salinity stresses (SR, dS/cm) (bottom) at the N application rate (NR) of 200 kg ha^{-1}.

Table 3
The best 10% and 25% combinations of N-application rates (NR, kg ha^{-1}) and irrigation levels (IL, %) for different salinity rates (SR, dS m^{-1}) under PRD and DI.

Irrigation strategy	Salinity rate (SR)	Optimal at the best 10%		Optimal at the best 25%	
		Optimal NR	Optimal IL	Optimal NR	Optimal IL
PRD	Low (SR ≤ 2)	100-200	70-90	100-300	50-100
	Low to intermediate (2 < SR ≤ 5)	100-200	60-90	50-250	50-100
	Intermediate to high (5 < SR ≤ 8)	100-150	50-80	50-200	50-90
	High (SR > 8)	50-150	40-70	50-200	30-80
DI	Low (SR ≤ 2)	100-200	80-100	100-200	60-100
	Low to intermediate (2 < SR ≤ 5)	100-150	70-90	50-200	60-100
	Intermediate to high (5 < SR ≤ 8)	50-100	60-90	50-150	50-90
	High (SR > 8)	50-100	40-70	50-150	30-80

applications above the rate of 200 kg ha^{-1} increased the risk of environmental deterioration as reflected by a linear increase in the *GWF* while it did not significantly improve the farm economics. Furthermore, crops exposed to low-intermediate salt and water deficit stresses performed better economically, which may indicate an enormous potential for reducing crops water footprint as well as the pollutant load to groundwater. Our results demonstrated that the PRD scenarios produced better results than the DI scenarios, suggesting that a sustainable agriculture may be easier achieved under PRD. It can be concluded that regional-specific benchmark levels for the total consumptive and degradative grey WFs that were developed while considering a wide-range of field management strategies can provide enough information to farmers to achieve higher income, save scarce blue water resources, and prevent agricultural-related environmental hazards by adjusting the fertilization and irrigation management as a function of the irrigation water salinity. Reliable estimations of these indices based on the results calculated by the HYDRUS (2D/3D) model (previously calibrated and validated against corresponding experimental data) indicate that this approach may represent an alternative approach to the labor- and time-consuming field investigations.

Acknowledgement

Fatemeh Karandish would like to thank the University of Zabol for financing the project (Grant Number: UOZ_GR_9517_6).

References

Ajdary, K., Singh, D.K., Singh, A.K., Khanna, M., 2007. Modelling of nitrogen leaching from experimental onion field under drip fertigation. Agr. Water Manage. 89, 15–28.
Aldaya, M.M., Martinez-Santos, P., Llamas, M.R., 2010. Incorporating the water footprint and virtual water into policy: reflections from the Mancha Occidental region, Spain. Water Resour. Manage. 24 (5), 941–958.
Assouline, S., Moller, M., Cohen, S., Ben-Hur, M., Grava, A., Narkis, K., Silber, A., 2006. Soil–plant system response to pulsed drip irrigation and salinity: bell pepper-case study. Soil. Sci. Soc. Am J. 70, 1556–1568.
Azizian, A., Sepaskhah, A.R., 2014a. Maize response to differet water, salinity and nitrogen levels: agronomic behavior. Int. J. Plant Prod. 8 (1), 107–130.
Azizian, A., Sepaskhah, A.R., 2014b. Maize response to differet water, salinity and nitrogen levels: physiological growth parameter and gas exchange. Int. J. Plant. Prod. 8 (1), 131–162.
Burow, K.R., Nolan, B.T., Rupert, M.G., Dubrovsky, N.M., 2010. Nitrate in groundwater of the United States, 1991–2003. Environ. Sci. Technol. 44, 4988–4997.
Chukalla, A.D., Krol, M.S., Hoekstra, A.Y., 2017. Grey water footprint reduction in irrigated crop production: effect 1 of nitrogen application rate, nitrogen form, tillage practice and irrigation strategy. Hydrol. Earth Syst. Sci. Discuss. http://dx.doi.org/

10.5194/hess-2017-224. 2017.
Corwin, D.L., Rhoades, J.D., Šimůnek, J., 2007. Leaching requirement for soil salinity control: steady-state versus transient models. Agric. Water Manage. 90, 165–180.
Cote, C.M., Bristow, K.L., Charlesworth, P.B., Cook, F.J., Thorburn, P.J., 2003. Analysis of soil wetting and solute transport in subsurface trickle irrigation. Irrig. Sci. 22, 143–156.
Crevoisier, D., Popova, Z., Mailhol, J.C., Ruelle, P., 2008. Assessment and simulation of water and nitrogen transfer under furrow irrigation. Agric. Water Manage. 95 (4), 354–366.
Dahan, O., Babad, A., Lazarovitch, N., Russak, E.E., Kurtzman, D., 2014. Nitrate leaching from intensive organic farms to groundwater. Hydrol. Earth Syst. Sci. 18, 333–341.
Doltra, J., Munoz, P., 2010. Simulation of nitrogen leaching from a fertigated crop rotation in a Mediterranean climate using the EU-rotate N and Hydrus-2D models. Agr Water Manag 97, 277–285.
Dry, P.R., Loveys, B.R., 1998. Factors influencing grapevine vigor and the potential for control with partial root zone drying. Aust. J. Grape Wine Res. 4, 140–148.
Dudley, L.M., Ben-Gal, A., Lazarovitch, N., 2008. Drainage water reuse: biological, physical, and technological considerations for system management. J. Environ. Qual. 37, 25–35.
FAO, 2015. Food and Agriculture Organization of the United Nations. Rome, Italy. http://www.fao.org/faostat/en/.
Feddes, R.A., Kowalik, P.J., Zaradny, H., 1978. Simulation of field water use and crop yield. Simulation Monographs. Pudoc, Wageningen.
Fort, C., Fauveau, M.L., Muller, F., Label, P., Granier, A., Dreyer, E., 1997. Stomatal conductance, growth and root signaling in young oak seedlings subjected to partial soil drying. Tree Physiol 17, 281–289.
Franke, N., Boyacioglu, H., Hoekstra, A., 2013. Grey water footprint accounting: tier 1 supporting guidelines. Value of Water Research Report Series No. 65. UNESCO-IHE, Delft, the Netherlands.
Gärdenäs, A.I., Hopman, J.W., Hanson, B.R., Šimůnek, J., 2005. Two-dimensional modeling of nitrate leahing for various fertigation scenarios under micro-irrigation. Agr Water Manage 74 (3), 219–242.
Gianquinto, G., Sambo, P., Pimpini, F., 2003. The use of SPAD-502 chlorophyll meter for dynamically optimising the nitrogen supply in potato crop. Acta Horti 627, 225–230.
Hanson, B.R., Šimůnek, J., Hopmans, J.W., 2006. Evaluation of urea-ammonium-nitrate fertigation with drip irrigation using numerical modeling. Agr Water Manag 86, 102–113.
Harter, T., Lund, J., 2012. Addressing nitrate in California& #8217;s drinking water with a focus on Tulare Lake Basin and Salinas Valley groundwater. Report for the State Water Resources Control Board Report to the Legislature. Centre for Watershed Sciences, University of California, Davis. http://groundwaternitrate.ucdavis.edu.
Haverkort, A.J., Vos, J., Booij, R., 2003. Precision management of nitrogen and water in potato production through monitoring and modeling. In: Proceedings of the XXVI International Horticultural Congress: Potatoes, Healthy Food for Humanity: International Developments in Breeding, Production, Protection and Utilization. Toronto, Canada.
Hoekstra, A.Y., Chapagain, A.K., Aldaya, M.M., Mekonnen, M.M., 2011. The Water Footprint Assessment Manual: Setting the Global Standard. Earthscan, London, UK.
Hu, T., Kang, Sh., Li, F., Zhang, J., 2009. Effects of partial root-zone irrigation on the nitrogen absorption and utilization of maize. Agric. Water Manage. 96, 208–214.
Hutson, J.L., Wagenet, R.J., 1991. Simulating nitrogen dynamics in soils using a deterministic model. Soil Use Manage. 7, 74–78.
Johnsson, H., Bergstrom, L., Jansson, P.-E., Paustian, K., 1987. Simulated nitrogen dynamics and losses in a layered agricultural soil. Agric. Ecosyst. Environ. 18, 333–356.
Kang, S.Z., Hu, X., Goodwin, I., Jerie, P., 2002. Soil water distribution, water use, and yield response to partial root zone drying under a shallow groundwater table condition in a pear orchard. Sci. Hortic. 92, 277–291.
Kang, S., Zhang, J., 2004. Controlled alternate partial root- Zone irrigation: its physiological consequences and impact on water use efficiency. J. Exp. Bot. 55, 2437–2446.
Karandish, F., 2016. Improved soil-plant water dynamics and economic water use efficiency in a maize field under locally water stress. Arch. Agron. Soil. Sci. http://dx.doi.org/10.1080/03650340.2015.1135326.
Karandish, F., Hoekstra, A.Y., 2017. Informing national food and water security policy through water footprint assessment: the case of Iran. Water 9 (11), 831. http://dx.doi.org/10.3390/w9110831. pp. 25.
Karandish, F., Shahnazari, A., 2016. Soil temperature and maize nitrogen uptake improvement under partial root zone drying. Pedosphere 26 (6), 872–886.
Karandish, F., Šimůnek, J., 2016a. A field-modeling study for assessing temporal variations of soil-water-crop interactions under water-saving irrigation strategies. Agric. Water Manage. 178, 291–303. http://dx.doi.org/10.1016/j.agwat.2016.10.009.
Karandish, F., Šimůnek, J., 2016b. Numerical and machine-learning modeling of soil water content for sustainable water management in agriculture under water stress. J. Hydrol. 543, 892–909. http://dx.doi.org/10.1016/j.jhydrol.2016.11.007.
Karandish, F., Šimůnek, J., 2017. Two-dimensional modeling of nitrogen and water dynamics for various n-managed water-saving irrigation strategies using HYDRUS. Agric. Water Manage. 193, 174–190. http://dx.doi.org/10.1016/j.agwat.2017.07.023. 2017.
Karandish, F., Darzi-Naftchali, A., Asgari, A., 2016. Application of machine-learning models for diagnosing health hazard of nitrate toxicity in shallow aquifers. Paddy Water Environ. http://dx.doi.org/10.1007/s10333-016-0542-2.
Kaya, Ç.I., Yazar, A., Sezen, S., 2015. SALTMED model performance on simulation of soil moisture and crop yield for Quinoa irrigated using different irrigation systems, irrigation strategies and water qualities in Turkey. Agric. Agric. Sci. Procedia 4, 108–118.
Kirda, C., Cetin, M., Dasgan, Y., Topcu, S., Kaman, H., Ekici, B., Derici, M.R., Ozguven, A.I., 2004. Yield response of greenhouse grown tomato to partial root drying and conventional deficit irrigation. Agric. Water Manage. 69, 191–201.
Kirda, C., Topcu, S., Kaman, H., Ulger, A.C., Yazici, A., Cetin, M., Derici, M.R., 2005. Grain yield response and N-fertiliser recovery of maize under deficit irrigation. Field Crops Res. 93, 132–141.
Klocke, N.L., Schneekloth, J.P., Melvin, S., Clark, R.T., Payero, J.O., 2004. Field scale limited irrigation scenarios for water policy strategies. Appl. Eng. Agric. 20, 623–631.
Li, J., Liu, Y., 2011. Water and nitrate distributions as affected by layered-textural soil and buried dripline depth under subsurface drip fertigation. Irrig. Sci. 29, 469–478.
Li, F., Liang, J., Kang, Sh., Zhang, J., 2007. Benefits of alternate partial root-zone irrigation on growth, water and nitrogen use efficiencies modified by fertilization and soil water status in maize. J. Plant Soil. 295, 279–291.
Li, Y., Šimůnek, J., Zhang, Z., Jing, L., Ni, L., 2015. Evaluation of nitrogen balance in a direct-seeded-rice field experiment using Hydrus-1D. Agric. Water Manage. 148, 213–222.
Liang, J., Zhang, J., Wong, M.H., 1996. Effects of air-filled soil porosity and aeration on the initiation and growth of secondary roots of maize (Zea mays). J. Plant Soil 186, 245–254.
Liu, F., Shahnazari, A., Andersen, M.N., Jacobsen, S.E., Jensen, C.R., 2006. Effects of deficit irrigation (DI) and partial root drying (PRD) on gas exchange, biomass partitioning, and water use efficiency in potato. Sci. Hortic. 109, 113–117.
Ma, L., Ahuja, L.R., Ascough II, J.C., Shaffer, M.J., Rojas, K.W., Malone, R.W., Cameira, M.R., 2001. Integrating system modeling with field research in agriculture: applications of the root zone water quality model (RZWQM). Adv. Agron. 71, 233–292.
Mer, R.K., Prajith, P.K., Pandya, D.H., Pandey, A.N., 2000. Effect of salts on germination of seeds and growth of young plants of Hordeum vulgare, Triticum aestivum, Cicer arietinum and Brassica juncea. J. Agron. Crop Sci. 185, 209–217.
Mguidiche, A., Provenzabo, G., Douh, B., Khila, S., Rallo, G., Boujelben, A., 2015. Assessing HYDRUS-2D to simulate soil water content (SWC) and salt accumulation under an SDI-system: application to potato crop in a semi-arid area of central Tunisia. Irrig. Drain. http://dx.doi.org/10.1002/ird.1884.
Monteny, G.J., 2001. The EU nitrates directive: a European approach to combat water pollution from agriculture. Sci. World J. 1, 927–935.
Mubarak, I., 2009. Effect of temporal variability in soil hydraulic properties on simulated water transfer under high-frequency drip irrigation. Agric. Water Manage. 96 (11), 1547–1559.
Nourbakhsh, F., Karimian Eghbal, M., 1997. Soil Fertility, 1st ed. Entesharat Ghazal. Isfahan. 312p. (In Farsi).
Paredes, P., Rodrigues, G.C., Alves, I., Pereira, L.S., 2014. Partitioning evapotranspiration, yield prediction and economic returns of maize under various irrigation management strategies. Agr Water Manage 135, 27–39.
Payero, J.O., Melvin, S.R., Irmak, S., Tarkalson, D., 2006. Yield response of corn to deficit irrigation in a semiarid climate. Agric. Water Manage. 84, 101–112.
Pereira, L.S., van den Broek, B., Kabat, P., Allen, R.G., 1995. Crop–Water Simulation Models in Practice. Wageningen Pers, Wageningen, The Netherlands. .
Phogat, V., Skewes, M.A., Cox, G., Alam, J., Grigson, G., Šimůnek, J., 2013. Evaluation of water movement and nitrate dynamics in a lysimeter planted with an orange tree. Agric. Water Manage. 127, 74–84 2013.
Phogat, V., Skewes, M.A., Cox, J.W., Sanderson, G., Alam, J., Šimůnek, J., 2014. Seasonal simulation of water, salinity and nitrate dynamics under drip irrigated mandarin (Citrus reticulata) and assessing management options for drainage and nitrate leaching. J. Hydrol. 513, 504–516.
Poni, S., Tagliavini, M., Neri, D., Scudellari, D., Toselli, M., 1992. Influence of root pruning and water stress on growth and physiological factors of potted apple, grape, peach and pear trees. Sci. Hortic. 52, 223–226.
Radcliffe, D.E., Šimůnek, J., 2010. Soil Physics With HYDRUS. CRC Press, Taylor & Francis Group, Boca Raton, FL, ISBN 978-1-4200-7380-5, pp. 373.
Ramos, T.B., Šimůnek, J., Gonçalves, M.C., Martins, J.C., Prazeres, A., Castanheira, N.L., Pereira, L.S., 2011. Field evaluation of a multicomponent solute transport model in soils irrigated with saline waters. J. Hydrol. 407, 129–144. http://dx.doi.org/10.1016/j.jhydrol.2011.07.016.
Ramos, T.B., Šimůnek, J., Goncalves, M.C., Martins, J.C., Prazeres, A., Pereira, L.S., 2012. Two-dimensional modeling of water and nitrogen fate from sweet sorghum irrigated with fresh and blended saline waters. Agric. Water Manage. 111, 87–104.
Raun, W.R., Solie, J.B., Johnson, G.V., Stone, M.L., Mullen, R.W., Freeman, K.W., Thomason, W.E., Lukina, E.V., 2002. Improving nitrogen use efficiency in cereal grain production with optical sensing and variable rate application. Agron. J. 94, 815.
Roberts, T., Lazarovitch, N., Warrick, A.W., Thompson, T.L., 2009. Modeling salt accumulation with subsurface drip irrigation using HYDRUS-2D. Soil Sci. Soc. Am. J. 73, 233–240.
Schachtman, D., Goodger, Q.D., 2008. Chemical root to shoot signaling under drought. Trend Plant. Sci. 13 (6), 281–287.
Self, J.R., Waskom, R.M., 2013. Nitrates in Drinking Water: Fact Sheet No. 0.517. Colorado State University Extension. http://www.ext.colostate.edu/pubs/crops/00517.pdf.
Sepaskhah, A.R., Ahmadi, S.H., 2010. A review on partial root-zone drying irrigation. Int. J. Plant. Prod. 4 (4), 241–258.
Sepaskhah, A.R., Kamgar-Haghighi, A.A., 1997. Water use and yields of sugar beet grown under every-otherfurrow irrigation with different irrigation intervals. Agric. Water Manage. 34, 71–79.
Shao, G.C., Zhang, Z.Y., Liu, N., Yu, S.E., Xing, W.G., 2008. Comparative effects of deficit irrigation (DI) and partial rootzone drying (PRD) on soil water distribution, water use, growth and yield in greenhouse grown hot pepper. Sci. Hortic. 119 (1), 11–16.
Shyns, J.F., Hoekstra, A.Y., 2013. The Water Footprint of Morocco and Its Added Value for National Water Policy. MSc Thesis. University of Twente.
Šimůnek, J., van Genuchten, M.Th., Šejna, M., 2008. Development and applications of the

HYDRUS and STANMOD software packages and related codes. Vadose Zone J. 7 (2), 587–600. http://dx.doi.org/10.2136/VZJ2007.0077.
Šimůnek, J., van Genuchten, M.Th., Šejna, M., 2011. Technical manual, version 2. PC progress, prague, Czech Republic. The HYDRUS Software Package for Simulating Two- and Three-Dimensional Movement of Water, Heat, and Multiple Solutes in Variably-Saturated Media. pp. 258.
Šimůnek, J., van Genuchten, M.Th., Šejna, M., 2016. Recent developments and applications of the HYDRUS computer software packages. Vadose Zone J. 15 (7), 25. http://dx.doi.org/10.2136/vzj2016.04.0033.
Siyal, A.A., Skaggs, T.H., 2009. Measured and simulated soil wetting patterns under porous clay pipe sub-surface irrigation. Agric. Water Manage. 96 (6), 893–904.
Skaggs, T.H., Shouse, P.J., Poss, J.A., 2006. Irrigating forage crops with saline waters: 2. Modeling root uptake and drainage. Vadose Zone J. 5, 824–837.
Stone, L.R., 2003. Crop water use requirements and water use efficiencies. In: Proceedings of the 15th Annual Central Plains Irrigation Conference and Exposition, Colby. Kansas. pp. 127–133.
Tafteh, A., Sepaskhah, A.R., 2012. Application of HYDRUS-1D model for simulating water and nitrate leaching from continuous and alternate furrow irrigated rapeseed and maize fields. Agric. Water Manage. 113, 19–29.
Tang, L.S., Li, Y., Zhang, J., 2005. Physiological and yield responses of cotton under partial root-zone irrigation. Field Crop Res. 94, 214–223.
Thompson, A.J., Andrews, J., Mulholland, B.J., McKee, J.M.T., Hilton, H.W., Horridge, J.S., Farquhar, G.D., Smeeton, R.C., Smillie, I.R.A., Black, C.R., Taylor, I.B., 2007. Overproduction of Abscisic acid in tomato increases transpiration efficiency and root hydraulic conductivity and influences leaf expansion. Plant. Physiol. 143, 1905–1917.
US Salinity Laboratory Staff, 1954. Diagnosis and Improvement of Saline and Alcaly Soils. USDA Handbook 60. Washington, USA. .
Vale, M., Mary, B., Justes, E., 2007. Irrigation practices may affect denitrification more than nitrogen mineralization in warm climatic conditions. Biol. Fertil. Soils 43, 641–651.
van Genuchen, M.Th., 1987. A numerical model for water and solute movement in and below the root zone. Res. Rep. 121 US Salinity Laboratory, USDA, ARS, Riverside, California.
Varvel, G.E., Schepers, J.S., Francis, D.D., 1997. Ability for in-season correction of nitrogen deficiency in corn using chlorophyll meters. Soil. Sci. Soc. Am. J. 61, 1233–1239.
Wang, H., Liu, F., Andersen, M.N., Jensen, C.R., 2009. Comparative effects of partial root-zone drying and deficit irrigation on nitrogen uptake in potatoes (solanum tuberosum L.). Irrig Sci. J. 27, 443–448.
Wang, H., Ju, X., Wei, Y., Li, B., Zhao, L., Hu, K., 2010. Simulation of bromide and nitrate leaching under heavy rainfall and high-intensity irrigation rates in North China Plain. Agric. Water Manag. 97, 1646–1654.
Wang, Z., Liu, F., Kang, Sh., Jensen, C.R., 2012. Alternate partial root-zone drying irrigation improves nitrogen nutrition in maize (Zea mays L.) Leaves. J. Environ. Exp. Bot. 75, 36–40.
Yazdani, V., Davari, K., Ghahreman, B., Kafi, M., 2004. Assesment of the water –salinity production function models –Canola application in the Mashhad area. J. Irrig. Water Manage. 5 (18), 32–53 In Persian.
Yurtseven, E., Sönmez, B., 1992. Sulama Sularının Değerlendirilmesi, Tarım Ve Köy İşl.Bk., KHGM, Toprak Ve Gübre Araşt. Enst. Md. Yayınları No.181/T-63, 62s. Ankara. .
Zeng, W., Xu, C., Wu, J., Huang, J., 2014. Soil salt leaching under different irrigation regimes: HYDRUS-1D modelling and analysis. J. Arid Land. 6 (1), 44–58.
Zhu, J.H., Li, X.L., Christie, P., Li, J.L., 2005. Environmental implications of low nitro-gen use efficiency in excessively fertilized hot pepper (capsicum frutescens L.) Cropping systems. Agric. Ecosyst. Environ. 111, 70–80.